PHILOSOPHICAL TRANSACTIONS OF THE ROYAL SOCIETY A MATHEMATICAL, PHYSICAL & ENGINEERING SCIENCES

Star Formation in a Galactic Cluster

M. M. Woolfson

Phil. Trans. R. Soc. Lond. A 1979 **291**, 219-252
doi: 10.1098/rsta.1979.0022

STAR FORMATION IN A GALACTIC CLUSTER

By M. M. WOOLFSON

Physics Department, University of York, Heslington, York YO1 5DD, U.K.

(*Communicated by W. H. McCrea, F.R.S. – Received* 9 *March* 1978
– *Revised* 15 *June* 1978)

CONTENTS

A model has been developed for the collapse of an interstellar cloud with turbulence. The differential equations which describe the evolution of the cloud include ionic and dust cooling and also the dissipation of energy due to the collision of turbulent elements moving at supersonic speeds. Under some conditions the collision of two elements can give rise to a star and the rate of star formation and the mass of the stars formed changes as the cloud collapses. The pattern found is that the stars first produced have masses of about 1.4 $M_{\odot}$ and the masses get less as star formation continues. Stars produced by this mechanism have little associated angular momentum. Some of the stars which happen to move in high density regions of the cloud may increase their mass greatly by accretion; these stars will be the more massive stars and they will also rotate most rapidly, a theoretical prediction which agrees with observation. On the basis of the model the proportion of stars which would have planetary systems is estimated. This shows that there should be of order 10^6 planetary systems per galaxy.

1. Introduction

Important contributions have been made to the topic of star formation by, amongst others, Hayashi (1961), Bodenheimer (1968), Larsen (1969), Disney, McNally & Wright (1969) and Hattori, Nakano & Hayashi (1969). This, and other work related to stellar evolution, is the subject of review papers by Hayashi (1966), Tayler (1968), McNally (1971) and Bodenheimer (1972).

Much of this activity has been concerned with the evolution of protostars. The starting point for such studies is a sphere of gas and dust of mass 0.1–10 $M_{\odot}$ or more at density typically 10^{-15} kg m^{-3} and temperature mostly in range 8–50 K. These studies show that initially the contraction is almost free-fall, with cooling by dust grains and perhaps also by the excitation and ionization of various molecules and atoms. As the collapse proceeds to higher densities so the opacity of the protostellar material increases leading to a build up of temperature and pressure within the protostar. Eventually the star reaches a state of quasi-equilibrium where the collapse rate is governed by the rate at which it radiates energy. The internal temperature rises until nuclear processes are initiated and soon thereafter the star enters its main-sequence stage.

While there are differences of detailed approach by various workers, there is general agreement about the important features and the final outcome, a star on the main sequence, is common to all such theories.

Less attention has been paid to the way in which the protostar comes into being in the first place. The basic ingredient for protostar formation is interstellar material with density 10^{-21} kg m^{-3}. The first stage in the process is the separation of clouds of density significantly higher than the background interstellar density. An indication of how this could come about has been given by Field, Goldsmith & Habing (1969). Since the heating of the interstellar medium by cosmic rays is independent of density and temperature but cooling processes are both density and temperature dependent then for stable thermal equilibrium at a given pressure there exist two sets of conditions, one of lower density and higher temperature and the other of higher density and lower temperature. This is a bistable system; with the background interstellar medium as the lower density, higher temperature region, then some influence, such as a slight excess of dust in a particular volume of space, could trigger off the formation of a higher density and lower temperature region. Such a region, once formed, may be capable of spontaneous collapse under self-gravitational forces if its total mass exceeds the critical value indicated by Jeans's criterion (Jeans 1902).

The problem of the separation of a protostar from the collapsing cloud has given rise to a number of different ideas. Hoyle (1953) described the process of fragmentation of a collapsing interstellar cloud based on the idea that as the density increased so smaller masses were required to satisfy Jeans's criterion. A hierarchy of fragmentation processes would eventually lead to stellar size collapsing cloudlets, which would be identified as protostars. This simple view of fragmentation was challenged by Layzer (1964) who argued that, since the fragments would have the same density as the cloud as a whole, the free fall time of the subunits and of the complete cloud would be the same and that no separation into stars would result. This result has, in turn, been disputed by Disney, McNally & Wright (1969) who have studied the linear wave flow collapse of an interstellar cloud by numeral analysis. These workers have shown that any small density perturbation would grow, a conclusion agreeing with that of Hunter (1962, 1964), and they conclude that a collapsing cloud has an inherent tendency to fragment.

There should also be mentioned the important ideas contained in McCrea's (1960) floccule theory for the formation of planetary systems. McCrea considered as of central importance the observed slow rotation of the sun and of many late type stars. In the floccule model the collapsing cloud is represented by a large number of high-density regions of about planetary mass moving randomly in less-dense background material. These floccules coalesce when they collide and with reasonable values for various parameters of the model it was shown that, due to the operation of $\sqrt{n}$ statistics, a resulting star of solar mass would have angular momentum consistent with observation. Small aggregations of floccules left in orbit around the central star would give rise to a planetary system. In McCrea's model the randomly moving floccules represent turbulence within the collapsing cloud.

Another interesting piece of work involving fragmentation, albeit on a galactic scale, is due to Grzedzielski (1966). The fragmentation of a pre-galaxy is described in terms of the effects of random plane shock waves which compress material to densities at which it can spontaneously collapse.

In this paper echoes of McCrea's and Grzedzielski's work will be detected.

2. Observational background

Clusters of stars are of two distinct types: globular clusters containing 10^5–10^6 stars and galactic clusters with 10^2–10^3 members. Individual stars occasionally leave clusters and a typical lifetime for a galactic cluster is in the range 0.1–1 Ga (Chandrasekhar 1960). Whilst it cannot be stated with certainty that all stars, or even most stars, are born in clusters, the presence of many thousands of clusters of stars show that there exist conditions which are conducive to the formation of stars in associations.

Once a star reaches the main sequence its appearance and properties are virtually constant over a long span of time. However in a young cluster, where many stars are in a pre-main-sequence stage and developing rapidly, it is possible to infer something about the timescale and sequence of events in the processes of star formation. Hayashi (1961) has calculated theoretical tracks of pre-main-sequence stars of various masses on the Hertzsprung–Russell diagram, and positions on the H.-R. diagram correspond to a unique mass and age. Making use of these tracks Iben & Talbot (1966) and Williams & Cremin (1969) have analysed the observational data from a number of young stellar clusters. The conclusions of the latter workers are illustrated in figure 1. In figure 1*a* the mass-age correlation for the galactic cluster NGC 2264 is shown and the clusters NGC 6530, IC 2602 and IC 5146, give similar results. The earliest stars are of mass somewhat above one solar mass and, later, stars both less and more massive are formed. Two streams of development with a period of bifurcation about 5 Ma ago seem to be indicated. Another deduction from figure 1*a* is that the rate of star formation is slow at first but steadily increases with time. A smoothed-out age to frequency diagram is shown in figure 1*b*. A final relation which we may note in figure 1*c* is the mass function, $f(M)$, the number of stars per unit mass range. Except for low masses the distribution appears to be:

$$f(M) \propto M^{-2.5}, \tag{1}$$

and the mass index agrees tolerably well with the value usually quoted of about -2.3.

While there may be some uncertainties about the results quoted by Williams & Cremin, which

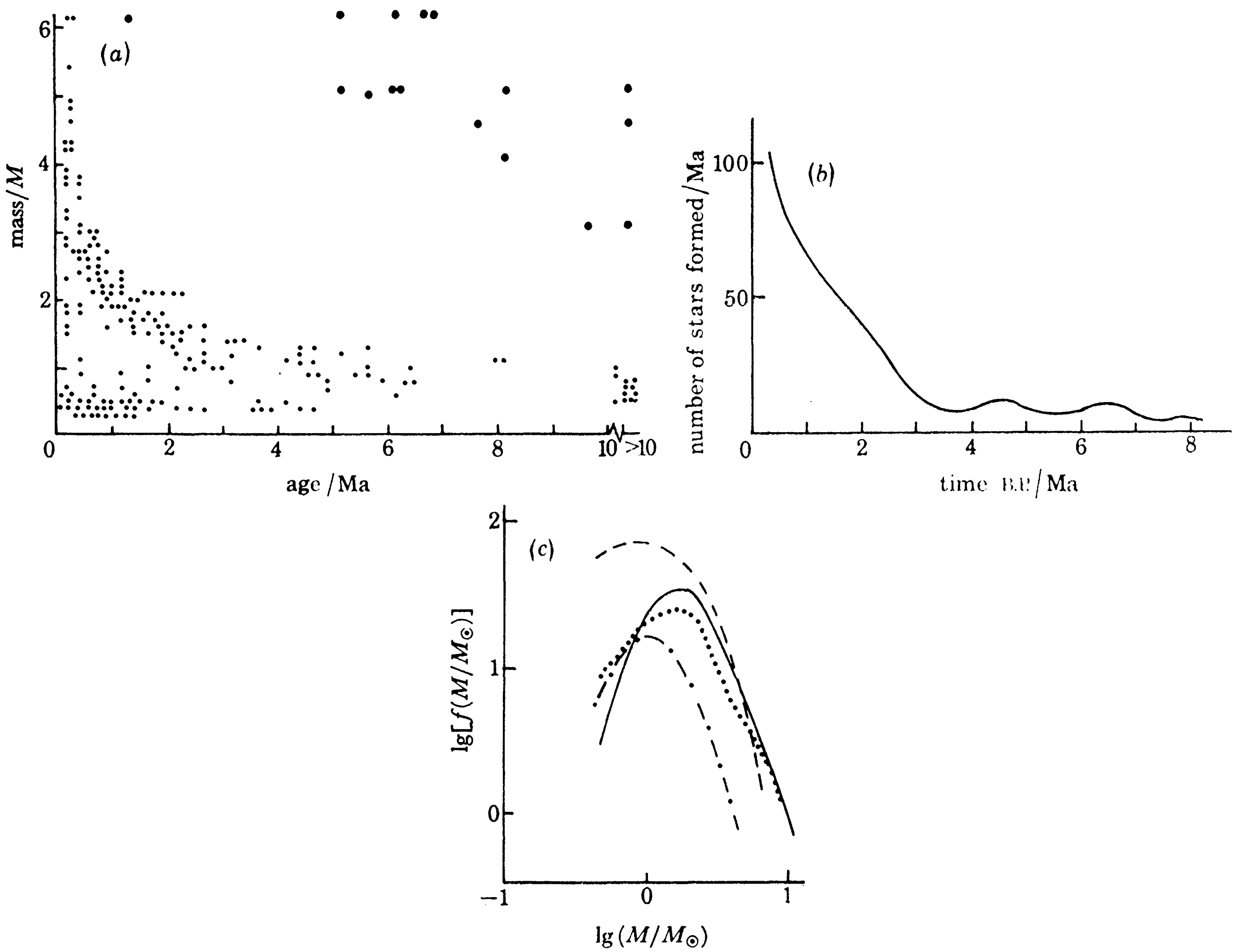

FIGURE 1. (*a*) Stellar mass against age for the cluster NGC 2264. (*b*) The rate of star formation for NGC 2264. (*c*) The mass distribution function for: ——, NGC 6530; —·—, IC 5146; ----, NGC 2264; ...., IC 2602.

are dependent on the assumed theoretical model, there seems to be little doubt about the general sequence of events in star formation in a galactic cluster which a satisfactory theory would need to explain.

3. The collapse of a cloud with turbulence

It must be stated at the outset that the model is presented with many simplifying assumptions. As a first approach, the philosophy followed was to remove all possible complications in order to obtain a feeling for the rôle that various features were playing before attempting any more complicated modelling. In the event, the results obtained seemed sufficiently interesting and significant to be presented in their own right before further analysis was attempted.

We start with a homogeneous spherical, non-rotating cloud of gas, with some turbulence, in a state of uniform homologous collapse. The cloud parameters are: mass M, radius R, temperature θ, radial speed of surface material $\dot{R}$ and mean-square turbulent speed u^2 $(=\epsilon)$.

The virial theorem gives:

$$\tfrac{1}{2}\ddot{I} = 2T_l + 2T_t + 3(\gamma - 1)U + \Omega \qquad (2)$$

where, for a uniform sphere, the moment of inertia about the centre of mass

$$I = \tfrac{3}{5}MR^2, \tag{3}$$

T_l and T_t are the kinetic energies associated with linear wave flow motion and turbulent motion respectively, U is the internal energy of the gas, γ the usual ratio of specific heats and Ω the total potential energy of the sphere given by

$$\Omega = -\tfrac{3}{5}GM^2/R. \tag{4}$$

For the sphere in uniform collapse

$$T_l = \tfrac{3}{10}M\dot{R}^2 \tag{5}$$

and we also have

$$T_t = \tfrac{1}{2}M\epsilon. \tag{6}$$

The remaining term on the right hand side of (2) is twice the translational component of the internal energy given by

$$3(\gamma-1)\,U = 3Mk\theta/m \tag{7}$$

where k is Boltzmann's constant and m the mass of a gas molecule.

Substitution from equations (3) to (7) into equation (2) gives

$$\ddot{R} = 5\frac{k\theta}{mR}+\frac{5\epsilon}{3R}-\frac{GM}{R^2}. \tag{8}$$

The first two terms on the right hand side of equation (8) represent thermal pressure and turbulent pressure forces which inhibit the collapse of the cloud, while the final term is the self-gravitational force which tends to induce collapse.

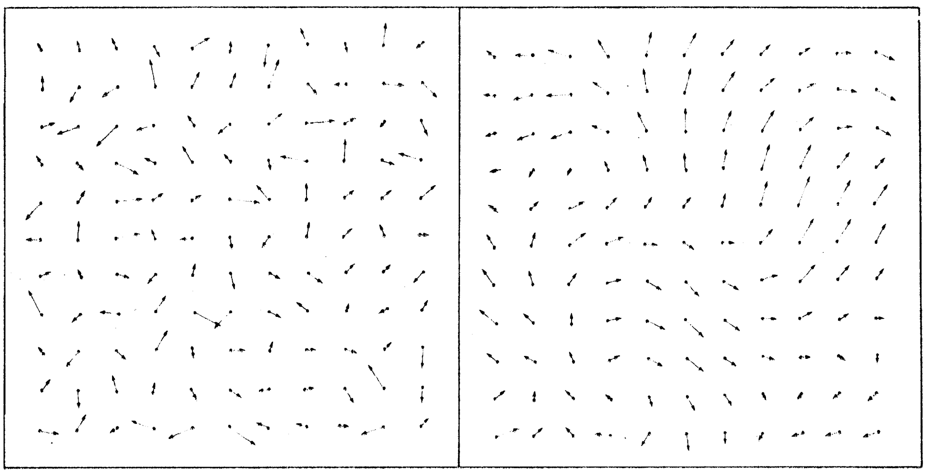

(*a*) (*b*)

FIGURE 2. (*a*) Velocities chosen randomly from a Maxwellian distribution on a two-dimensional grid. (*b*) After three stages of 'velocity sharing' local correlation has been introduced.

4. A MODEL OF TURBULENCE

The next part of the analysis involves energy transfer within the cloud and between the cloud and the environment. However, we must first consider how turbulence is to be modelled. Figure 2*a* represents a random velocity field, with Maxwellian distribution, in two dimensions. The velocity at each point is replaced by a weighted average of itself and the velocity at all surrounding points with a weight which falls off with distance (Aust 1973). After three stages of the same process we obtain the velocity field shown in figure 2*b*. The effect has been to introduce local correlation; this leads to the idea of a correlation distance and what is proposed here is that this is strongly related to the Jeans diameter corresponding to the density and temperature of the cloud.

The actual model used for turbulence is to consider the whole sphere of gas as a conglomerate of closely packed spheres, each with the Jeans radius R_J. All spheres, considered as turbulent elements, are taken as having the same speed, u, with respect to the local average velocity, but in a random direction.

5. The turbulence equation

We shall now be concerned with the way in which gravitational potential energy is transformed into other forms of energy.

As the cloud collapses so there will be changes in Ω, T_1 and T_t with gravitational energy feeding the other two. Some turbulent energy is dissipated in the collision of turbulent elements at a rate Q_t per unit mass. A further part of the gravitational energy does work in compressing the cloud material and for homologous collapse the rate of doing such work per unit mass is readily found to be

$$Q_1 = -\frac{3k\theta}{mR}\dot{R}. \tag{9}$$

We may now write the equation for energy conservation as

$$\dot{\Omega} + \dot{T}_1 + \dot{T}_t + M(Q_1 + Q_t) = 0 \tag{10}$$

or

$$\frac{3GM^2}{5R^2}\dot{R} + \tfrac{3}{5}M\dot{R}\ddot{R} + \tfrac{1}{2}M\dot{\epsilon} - \frac{3Mk\theta}{mR}\dot{R} + MQ_t = 0.$$

Substituting for $\ddot{R}$ from equation (8) gives

$$\dot{\epsilon} = -\frac{2\epsilon}{R}\dot{R} - 2Q_t. \tag{11}$$

In order for turbulence to be generated within a collapsing cloud there must be some turbulence present in the first place. Such initial turbulence may be induced in an interstellar cloud by an external influence, for example radiation from nearby stars, an inter-cloud collision or a supernova explosion.

6. Energy loss by turbulent collisions

It will be found later that, for all but a short period, the turbulence will be supersonic. Figure 3 illustrates the head-on collision of two turbulent streams at a plane interface. The speed of the oncoming streams is w and a shockfront travels back from the interface into each stream at a speed v, the material being compressed and heated in the process.

The timescale for cooling of the heated material is too long to affect the process of shock compression (Kaplan 1966) but cooling does take place quite quickly after the passage of the shock wave. Indeed, in a private communication Aust (1978) asserts that, owing to the density dependence of cooling processes, the compressed material eventually cools to a temperature *below* that before compression. After compression the turbulent elements re-expand to their original density (or nearly so) but comparatively slowly and isothermally. By adapting some results due to Aust (1974) the loss of energy per unit mass in compression plus reexpansion may be shown to be

$$E_t = \frac{k\theta}{m}\left\{\frac{1}{2\gamma}\left[\left(\frac{v}{c}\right)^2 + 2\frac{wv}{c^2}\right] - \ln\left(\frac{\rho_2}{\rho_1}\right)\right\} \tag{12}$$

where
$$\frac{v}{c} = -\left(\frac{3-\gamma}{4}\right)\frac{w}{c} + \left[\left(\frac{\gamma+1}{4}\right)^2\frac{w^2}{c^2} + \gamma\right]^{\frac{1}{2}}, \tag{13}$$

$$\rho_2/\rho_1 = (v+w)/v, \tag{14}$$

and c is the speed of sound in the uncompressed material.

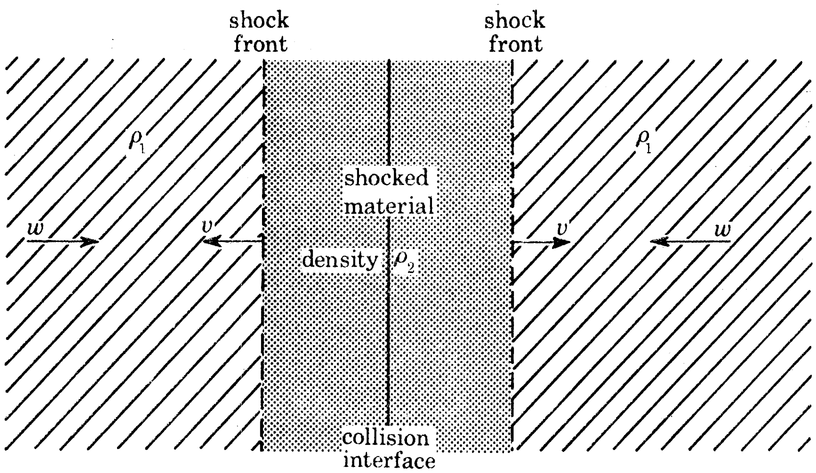

FIGURE 3. Material moving towards the collision interface at supersonic speed w produces shockfronts moving at speed v. The material is compressed from density ρ_1 to density ρ_2 by the collision of the turbulent streams.

A characteristic timescale for collisions, t_c, may be defined, which is the average interval between the involvement of any element of material in successive collisions. The rate of loss of thermal energy per unit mass then becomes

$$q_t = E_t/t_c. \tag{15}$$

If all the turbulent elements in the collapsing cloud collided head-on in pairs then, with $w = u$, q_t would give the quantity Q_t in equation (11). In practice there would be oblique and multiple collisions but the rate of loss of energy should be of the same order as q_t and we write

$$Q_t = \beta q_t, \tag{16}$$

where β is a constant representing the uncertainty of the collision timescale and also the validity of the pairing-off assumption.

7. TEMPERATURE CHANGES WITHIN THE CLOUD

When the cloud is collapsing there will be several sources of heat within it. Internal sources include linear wave flow compression of the gas, the heat generated by turbulent collisions, and radiation from the stars which have been produced in the cloud. Finally there are external sources which include the background starlight and also cosmic ray heating.

Cooling processes have been considered by many workers in great detail (see for example Gaustad 1963, Hayashi 1966, Disney, McNally & Wright 1969, Hattori, Nakano & Hayashi 1969). At all temperatures cooling by solid grains will be effective and, indeed, if for some reason the gas cools down to a temperature below that of the grains then the grains will become a heating agent.

The other type of cooling is by the excitation of various ions, C^+, Si^+, Fe^+ and Mg^+, by electron collision and by the excitation of atomic oxygen or molecular hydrogen by atomic collisions. At the temperatures of interest in the present work the oxygen cooling rate is unknown and H_2 cooling may be ignored.

The ionic cooling was given by Seaton (1955) in the form

$$Q_i = 1.79\times10^{14}\rho\theta^{-\frac{1}{2}}\{0.58\exp(-92/\theta)+5.0\exp(-413/\theta) + 1.7\exp(-554/\theta)+2.2\exp(-961/\theta)\}\,\mathrm{J\,kg^{-1}\,s^{-1}}, \quad (17)$$

where, at the temperatures of interest in this study, the first term in the bracket, due to C^+ cooling, is the dominant one. McNally (1971) has expressed some doubt about the validity of this equation at very low temperatures since the atoms providing the necessary ions may then be locked up in solid grains.

Grain cooling assumes that the grains are at a constant temperature θ_g and that gas molecules which strike a grain arrive and leave with energies $k\theta/(\gamma-1)$ and $k\theta_g/(\gamma-1)$ respectively (in Hayashi's 1966 paper these were taken as $k\theta$ and $k\theta_g$). With number densities of hydrogen atoms and molecules n_1 and n_2 it can be shown that the cooling rate per unit mass is

$$Q_g = \frac{kn_g r_g^2}{\rho}\left\{\frac{n_1}{(\gamma_1-1)\sqrt{m_1}}+\frac{n_2}{(\gamma_2-1)\sqrt{(2m_1)}}\right\}(8\pi k\theta)^{\frac{1}{2}}(\theta-\theta_g), \quad (18)$$

where n_g and r_g are the number density and mean radius of the grains, ρ the density of the gas and m_1 is the mass of a hydrogen atom. Values given by Gaustad (1963) and Hayashi (1966) are

$$r_g = 0.2\,\mu\mathrm{m} \quad \text{and} \quad n_g = 10^{-13}\frac{\rho}{m_1}.$$

We write for the cosmic ray heating rate per unit mass, Q_c, for ionic and grain cooling combined per unit mass, Q_{gi}, and for the rate of input of energy from stars and protostars, W_s. With the inclusion of compressional heating and heat produced by turbulent dissipation we find

$$Mk\left\{\frac{\mu}{m_1(\gamma_1-1)}+\frac{1-\mu}{2m_1(\gamma_2-1)}\right\}\dot{\theta} = -\frac{3Mk\theta}{\bar{m}R}\dot{R}+W_s+M(Q_t+Q_c-Q_{gi}), \quad (19)$$

where μ is the proportion by mass of atomic hydrogen in the cloud and where the m which appears in equation (8) is replaced by

$$\bar{m} = \left\{\frac{\mu}{m_1}+\frac{1-\mu}{2m_1}\right\}^{-1} = \frac{2m_1}{1+\mu}. \quad (20)$$

At this point we note an important simplification. At sufficiently high temperatures the γ values for atomic hydrogen and molecular hydrogen are $\frac{5}{3}$ and $\frac{7}{5}$ respectively. At low temperatures, lower than 20 K or so, the specific heat capacity of H_2 falls to $\frac{3}{2}R$, the same as the value for atomic hydrogen since rotational degrees of freedom cease to be involved in the internal energy.

With $\gamma_1 = \gamma_2 = \frac{5}{3}$ we find from (19) and (20)

$$\dot{\theta} = -\frac{2\theta\dot{R}}{R}+\frac{2\bar{m}}{3k}\left(\frac{W_s}{M}+Q_t+Q_c-Q_{gi}\right). \quad (21)$$

One factor which still needs to be included before equations (8), (11) and (21) can be solved is to allow for the mass of gas which is taken out of the cloud to form protostars. Once a protostar is formed the only coupling that exists with the surrounding material is through gravitation and its radiation as given by the quantity W_S. However, assuming that all stars stay within the cloud, we can allow for star formation by replacing M in the last term of equation (8) by M^2/M_G, where M_G is the mass of gaseous material, and by replacing M in equation (21) by M_G.

The analysis for the rate of change of temperature is included here for the sake of completeness but in the calculations which follow a constant temperature has been assumed. With both ionic and grain cooling, when the density is sufficiently high, say $10^{-17}\,\mathrm{kg\,m^{-3}}$, the temperature remains fairly constant. This temperature depends on cosmic ray heating, which is uncertain by about two orders of magnitude, on ionic and atomic coolants, uncertain both in concentration and effectiveness and on grain cooling, which depends on the grain temperature.

A potentially important source of heating is the formation of hydrogen molecules on the surfaces of solid grains. However, for this to occur grain temperatures of 7 K or less are required (Solomon & Wickramasinghe 1969) which is below the grain temperatures assumed in this paper and by most other workers. Since H_2 formation is temperature sensitive it will tend to be a self-regulating phenomenon. Excessive heat production by H_2 formation would raise the temperature of the grains which would then inhibit further formation of molecules.

Again, no allowance has been made for the effect of opacity in the cloud. This affects the cosmic ray formation of ionic coolants and also the escape of heat energy formed within the cloud (Disney *et al.* 1969). In view of these uncertainties it seemed to contravene the spirit of the simple modelling being attempted here to include temperature variations. Instead an isothermal model has been used but calculations have been carried out at several different temperatures within the range 8–30 K to show that the model behaviour is not critically dependent on temperature (see appendix A).

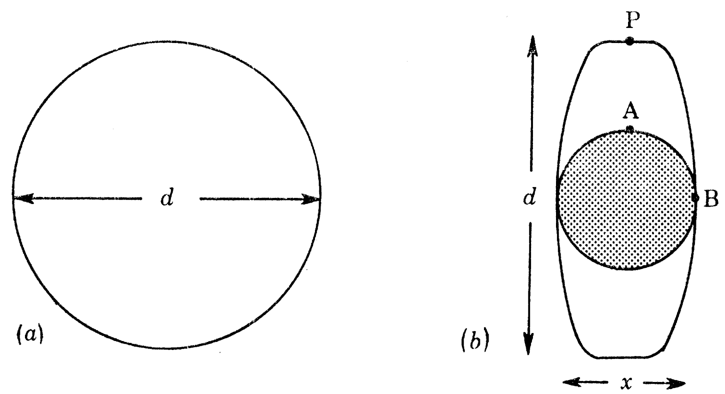

FIGURE 4. (*a*) A sphere of gas of diameter d which just satisfies Jeans's criterion. (*b*) The sphere compressed by a plane shock wave. The shaded region represents the largest sphere which may be inscribed within the compressed volume.

8. CONDITIONS FOR STAR FORMATION

In considering the role of turbulence in the fragmentation of a galaxy, Grzedzielski (1966) concluded that if a plane shock wave compressed a gaseous fragment which just satisfied Jeans's criterion then the fragment would not be induced to collapse. Figure 4*a* represents a spherical mass of diameter d which just satisfies Jeans's criterion so that

$$\tfrac{1}{2}d = \tfrac{1}{5}GM\overline{m}/k\theta, \tag{22}$$

where M is the total mass of gas and $\bar{m}$ is the average mass of a gas molecule. If the diameter is greater than d, other quantities being unchanged, then the sphere will expand.

The effect of compression by a plane wave is seen in figure 4*b*. Grzedzielski asserts that the behaviour of the compressed region depends on the mass and radius of the spherical portion, shown shaded, of diameter x. Since the radius is decreased by a factor x/d and the mass by $(x/d)^3$ it follows from equation (22) that the compressed gas will reexpand. Grzedzielski then shows that it would require the concerted action of at least three plane shock waves for the compressed region spontaneously to collapse.

It is important to stress the difference between Grzedzielski's model and the present one. Grzedzielski's shock wave is a disturbance which passes from one fragment to another, without causing the fragments to interact in any way. In the present model it is the turbulent motion of individual fragments which causes them to interact and so to generate shock waves within the material.

If two turbulent regions collide, even at very low velocity, then it might be thought that this will lead to a supracritical mass which will collapse to form a star of mass $2M_c$. In isolation this would be true but other factors have to be taken into account. Turbulent elements will be constantly breaking up and reforming and the coherence time for the turbulence pattern within the cloud will be of order t_c (see equation 15). Unless fragments appreciably collapse in a time t_c then their material will be restirred back into the cloud. This gives a lower limit for compression before a star can be formed.

There would also be an upper limit to compression if a Grzedzielski-type argument were involved. We now interpret figure 4*b* as the result of the collision of two spheres of material, each of diameter d. The compression of the gas is given by:

$$\phi = \frac{\text{original volume}}{\text{final volume}} = \frac{(8\pi/3)\,(\frac{1}{2}d)^3}{\pi(\frac{1}{2}d)^2 x} = \frac{4d}{3x}. \tag{23}$$

When we consider the behaviour of the cylindrical mass we shall be a little more precise than was Grzedzielski. Material at points, such as P, at the edge of the cylinder will move outwards and a rarefaction wave will move in towards the centre of the cylinder with the speed of sound. The material at point A at the surface of the shaded spherical volume will be initially stable, or at least will not move outwards. The critical point in assessing the stability of the whole spherical region is B. If this moves outwards then the gas will expand; otherwise it will contract and a protostar will form.

The gravitational field at B is due to the whole cylinder (not just the spherical region as Grzedzielski implies) and straightforward analysis shows this to be

$$E_B = \pi\rho_2 G d\left[1+\frac{2x}{d}-\sqrt{\left(1+\frac{4x^2}{d^2}\right)}\right], \tag{24}$$

where ρ_2 is the density of the compressed gas.

Substituting from (23) gives

$$E_B = \pi\rho_2 G d[1+\tfrac{8}{3}\phi^{-1}-\sqrt{(1+\tfrac{64}{9}\phi^{-2})}]. \tag{25}$$

If the shaded spherical volume alone was present as shown in figure 4*b* then the field would be

$$E'_B = \tfrac{2}{3}\pi\rho_2 G x. \tag{26}$$

The result for the whole cylinder at the point B is as though there was only the small shaded sphere but with its density increased by a factor E_B/E'_B. Hence, from (22) and (23), the condition that the mass should be able to collapse is

$$\tfrac{1}{2}x < \frac{G\overline{m}}{5k\theta}\,\tfrac{4}{3}\pi\rho_2\left(\frac{x}{2}\right)^3\frac{E_B}{E'_B},$$

or
$$2[1+\tfrac{8}{3}\phi^{-1}-\surd(1+\tfrac{64}{9}\phi^{-2})] > 1. \tag{27}$$

A solution of this equation gives

$$\phi < 3.6.$$

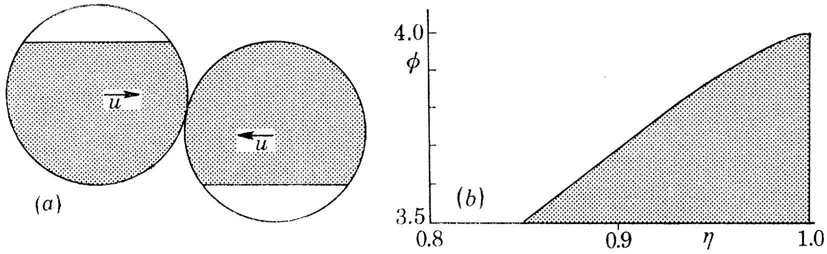

FIGURE 5. (*a*) The oblique collision of two turbulent elements, each of mass M_c, giving rise to the compression of the shaded material, mass $2\eta M_c$. (*b*) The shaded region giving values of ϕ and η which can give star formation.

While this analysis does give a figure for the upper limit of compression for the formation of a star it is only an approximate treatment. A constant temperature has been assumed, which can be defended on the grounds that the cooling time for the compressed gas is very much shorter than the reexpansion time (Hayashi 1966). Another factor, which favours collapse, is that the collision would give not a cylinder but rather a distribution of mass with greater concentration in the central region. For this reason, in numerical work, ϕ_{max} has usually been taken as 4.0 which may be thought of as coming from a modified inequality (27) in the form:

$$2[1+3\phi^{-1}-\surd(1+9\phi^{-2})] > 1. \tag{28}$$

A final situation which we consider is that of oblique collisions in which the compressed mass is less than $2M_c$. Figure 5*a* shows the relative motion of two colliding fragments relative to their combined centre of mass. The compressed material, of mass $2\eta M_c$, is shaded and the equation corresponding to (28) becomes

$$2\eta[1+3/\phi\eta-\surd(1+9/\phi^2\eta^2)] > 1, \tag{29}$$

which leads to
$$\eta > \tfrac{1}{4}(12-\phi)/(6-\phi). \tag{30}$$

In numerical work we have usually taken $\phi_{min} = 3.5$ which, inserted into (30) gives

$$\eta > 0.85. \tag{31}$$

We also find from (30) that

$$\phi < 12(2\eta-1)/(4\eta-1). \tag{32}$$

With $\eta = 0.85$ we find $\phi_{max} = \phi_{min} = 3.5$. For any higher value of η there is a range of values of ϕ giving star formation and this is shown in figure 5*b*.

With these considerations in mind we can now approach the problem of finding the rate at which stars are produced in the collapsing cloud.

PHILOSOPHICAL TRANSACTIONS OF THE ROYAL SOCIETY A MATHEMATICAL, PHYSICAL & ENGINEERING SCIENCES

9. The rate of star formation

We have seen that in order to obtain a star by the collision of two turbulent elements the compression factor, ϕ, must satisfy

$$\phi_{\min} \leqslant \phi \leqslant \phi_{\max}. \tag{33}$$

Now consider two neighbouring turbulent elements whose line of centres defines the x direction. Their velocities $\boldsymbol{u}_1$ and $\boldsymbol{u}_2$ have equal magnitudes and components with respect to a set of Cartesian axes (u_{x1}, u_{y1}, u_{z1}) and (u_{x2}, u_{y2}, u_{z2}). The velocities of the two bodies with respect to the combined centre of mass are

$$\pm\,\boldsymbol{w} = \pm\tfrac{1}{2}(u_{x1}-u_{x2}, u_{y1}-u_{y2}, u_{z1}-u_{z2}). \tag{34}$$

The angle, ψ, made by the vector $\boldsymbol{w}$ with the x direction is given by

$$\cos\psi = \tfrac{1}{2}|u_{x1}-u_{x2}|/|\boldsymbol{w}|. \tag{35}$$

We have taken the compressed volume (shaded in figure 5*a*) as a fraction $\cos\psi$ of the total mass of the two elements. Although this would not be true for spherical elements we recognize that our elements would be more cylindrical than spherical and the $\cos\psi$ fraction would then be more appropriate. In accordance with equation (31) this gives the condition that no star can be produced unless $\cos\psi > 0.85$.

The material which is to be compressed moves together as illustrated in figure 3 with speeds w; the corresponding ϕ is given by equation (14).

The directions of the vectors $\boldsymbol{u}_1$ and $\boldsymbol{u}_2$ are defined by angles (θ, ϕ) corresponding to a spherical polar coordinate system. From these angles and the value of u/c we determine whether or not the conditions for star formation are satisfied. We write

$$\begin{aligned} p(\theta_1, \phi_1, \theta_2, \phi_2) &= 1 \quad \text{if a star is formed (i.e. } \phi_{\min} < \phi < \phi_{\max}\text{), or} \\ &= 0 \quad \text{if a star is not formed.} \end{aligned}$$

Then the probability that a particular pair of interacting elements will produce a star is

$$P\left(\frac{u}{c}\right) = \int_0^{2\pi}\int_0^{\pi}\int_0^{2\pi}\int_0^{\pi} p(\theta_1, \phi_1, \theta_2, \phi_2)\sin\theta_1\sin\theta_2\,d\theta_1\,d\phi_1\,d\theta_2\,d\phi_2.$$

For very small u/c the quantity $p(\theta_1, \phi_1, \theta_2, \phi_2)$ will be zero for any direction of motion. For very large u/c there may be only a restricted range of angles for which (33) is satisfied and P will be correspondingly small. Figure 6 illustrates the variation of P with u/c for two values of γ and with different ranges of ϕ. It will be noted that for $\gamma = \frac{5}{3}$ and $\phi_{\max} = 4.0$ there is no maximum in the value of $P(u/c)$. When $(w/c) \to \infty$, $\phi \to (\gamma+1)/(\gamma-1)$ which is 4 when $\gamma = \frac{5}{3}$ and no matter how hard the collision one cannot obtain $\phi > \phi_{\max}$.

To estimate the number of stars produced per unit time we first assume that the turbulent elements interact in pairs. The number of turbulent elements, N, is M/M_c where

$$M_c = \tfrac{4}{3}\pi\rho R_J^3 \tag{37}$$

and, by modification of equation (22),

$$R_J = \left(\frac{15k\theta}{4\pi\bar{m}G\rho}\right)^{\frac{1}{2}}. \tag{38}$$

To estimate the characteristic timescale used in equation (15) we take the time for two turbulent elements of radius R_J to come together at a speed u, compress gas by a factor ϕ and then reexpand at the speed of sound, giving

$$t_c = 2R_J(1-1/\phi)\,(1/c+1/u). \tag{39}$$

The rate of star formation now becomes

$$\frac{dS}{dt} \approx \tfrac{1}{2}N\beta' P(u/c)/t_c \tag{40}$$

where the factor β', which describes a departure from the assumption of paired-off elements is similar in origin to β, as defined in equation (16), and is sometimes taken with the same value.

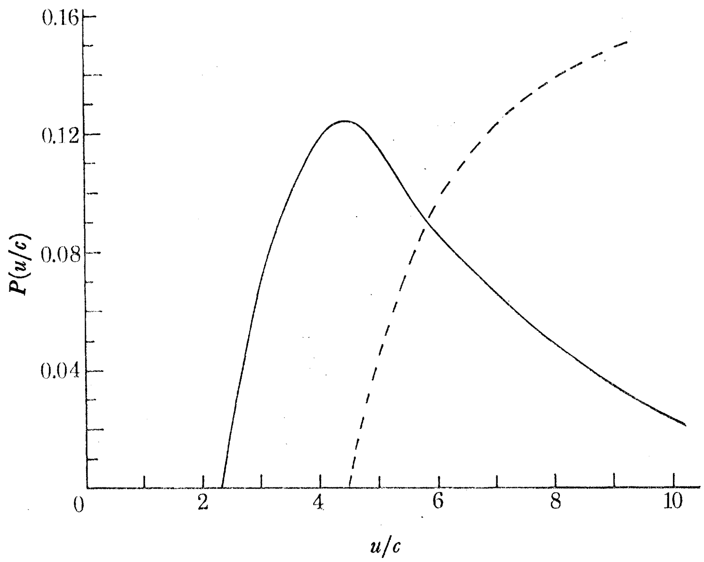

FIGURE 6. The probability function $P(u/c)$ for star formation;

——, $\gamma = 1.53$, $\phi_{min} = 3.0$, $\phi_{max} = 4.0$;
- - - -, $\gamma = \frac{5}{3}$, $\phi_{min} = 3.5$, $\phi_{max} = 4.0$.

However, the masses of the stars produced will not be $2M_c$. The mass we want is approximately that mass shown shaded in figure 4*b*, which is

$$M_s = \tfrac{4}{3}\pi\rho_2(x/2)^3 = 2M_c\frac{32}{27\phi^2}. \tag{41}$$

Thus with ϕ in the range 3.5–4.0 the mass of the star is of the order of 10% of the combined mass of the interacting turbulent elements.

10. NUMERICAL CALCULATIONS

The components for the numerical solution of the collapse of a cloud with turbulence and with star generation are now all assembled. The equations to be used are, for constant θ,

$$\ddot{R} = \frac{5k\theta}{\bar{m}R} + \frac{5\epsilon}{3R} - \frac{GM^2}{M_G R^2}, \tag{8'}$$

$$\dot{\epsilon} = -\frac{2\epsilon}{R}\dot{R} - 2Q_t, \tag{11}$$

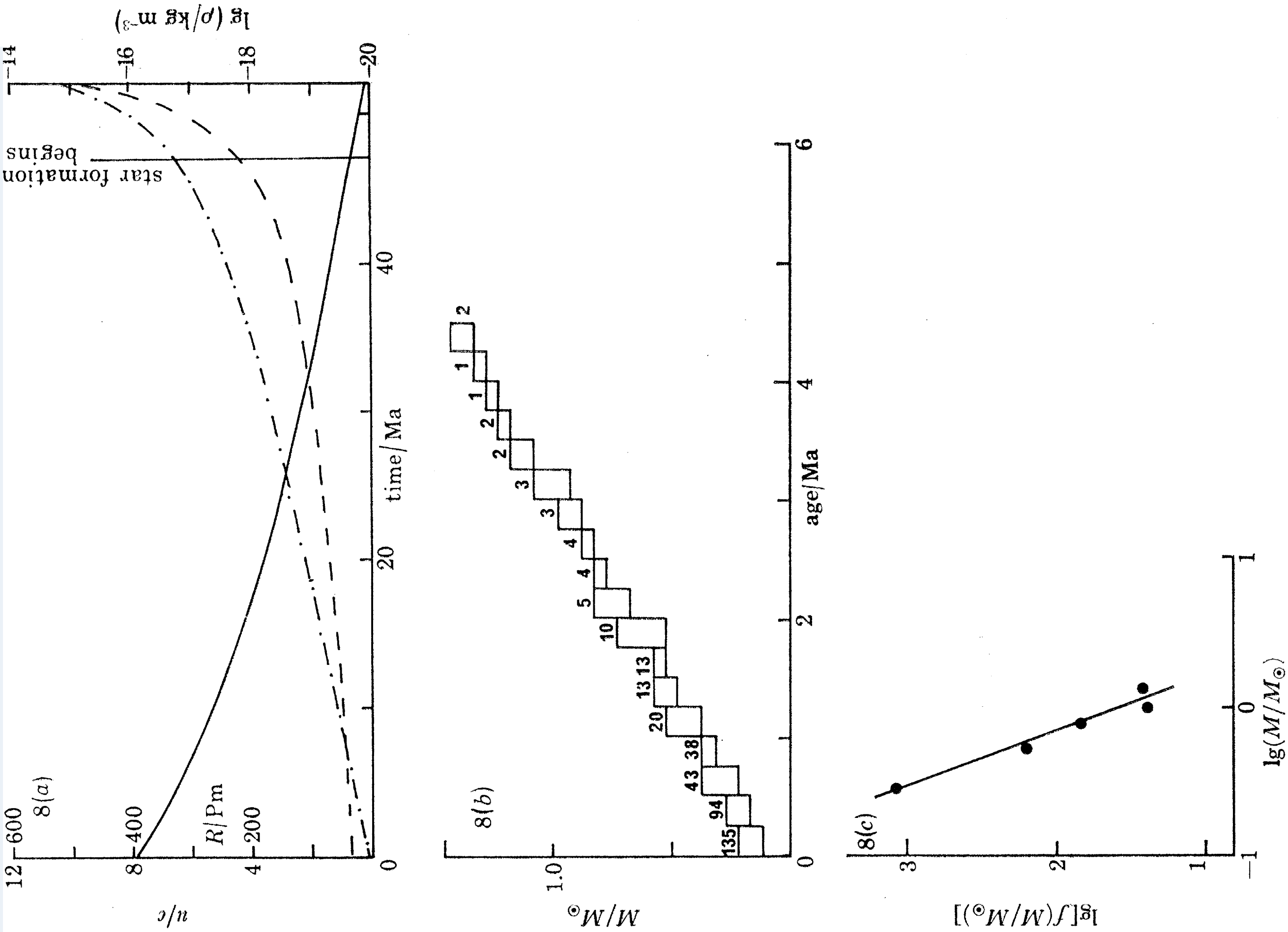

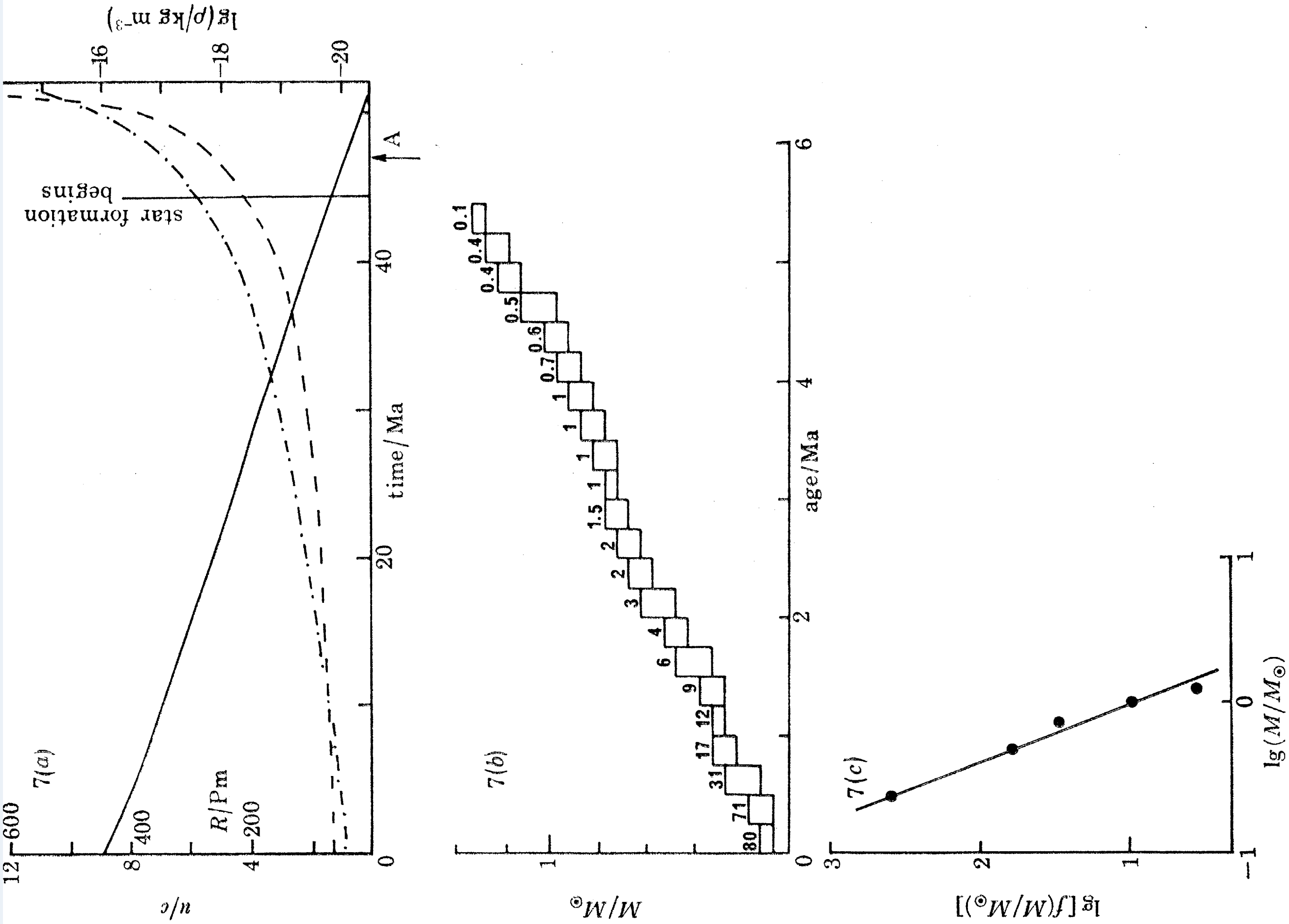

PHILOSOPHICAL TRANSACTIONS OF THE ROYAL SOCIETY A MATHEMATICAL, PHYSICAL & ENGINEERING SCIENCES

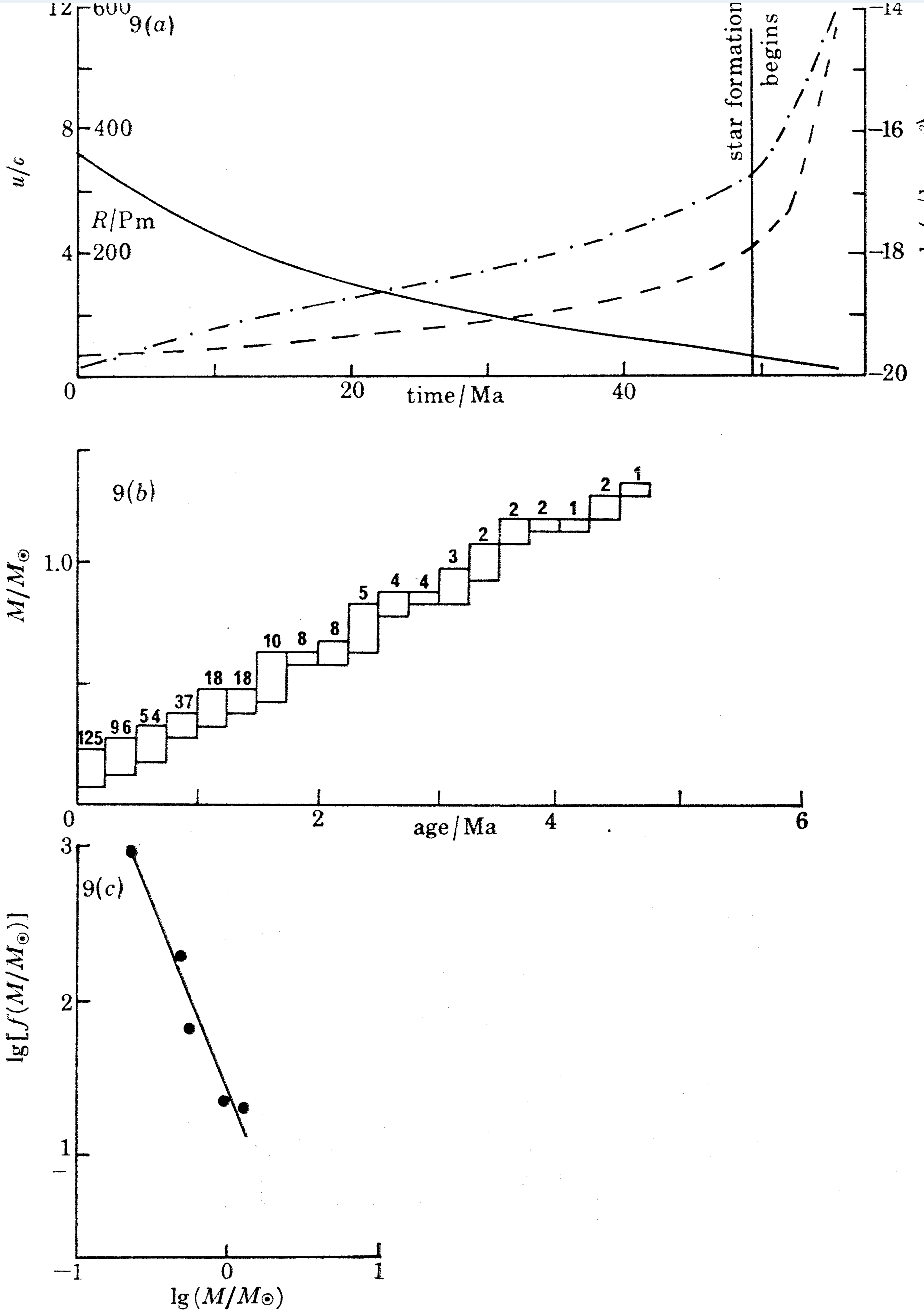

FIGURES 7, 8 AND 9. The collapse of a cloud with star formation. See table 1 for relevant parameters. Each figure depicts: (*a*) Variation with time of: ——, radius (R); - - - -, turbulence (u/c); -·-·-·-, density lg (ρ/kg m^{-3}). (*b*) Number of stars formed in intervals of 0.25 Ma, with the mass range of stars formed. (*c*) Frequency of star formation against mass. The slope of the line shown in figure 7*c* is −2.6, in figure 8*c* it is −2.7, and in figure 9*c* it is −2.5.

TABLE 1. PARAMETERS FOR THE CLOUD COLLAPSE AND STAR FORMATION CALCULATIONS ILLUSTRATED IN FIGURES 7, 8 AND 9.

	figure 7	figure 8	figure 9
mass of cloud/kg	3.0×10^{33}	3.0×10^{33}	3.0×10^{33}
temperature/K	8	20	30
γ	5/3	5/3	5/3
$\overline{m}$ (equation 22)/kg	2.0×10^{-27}	2.5×10^{-27}	3.22×10^{-27}
ϕ_{max}; ϕ_{min}(§8)	3.5; 4.0	3.5; 4.0	3.5; 4.0
β; β' (equations 16; 40)	1.0; 1.0	1.0; 1.0	1.0; 1.0
initial density/kg m^{-3}	8.2×10^{-21}	1.2×10^{-20}	1.5×10^{-20}
initial (dR/dt)/m s^{-1}	−325	−492	−527
initial u/c	1.24	0.71	0.66

and
$$\frac{dS}{dt} = \tfrac{1}{2}N\beta' P(u/c)/t_c. \tag{40}$$

The starting condition is a uniform cloud of composition fixed by the value of μ (equation 19) with a given mass, M, temperature, θ, and turbulence, ϵ_i. From μ we find $\bar{m}$, and the initial radius is chosen to correspond to density about 10^{-20} kg m^{-3}. The initial collapse speed $\dot{R}$ is chosen so that:
$$\tau_1 \approx \tau_t. \tag{42}$$

The pattern of events is not very critically dependent on starting conditions, except that with too little initial turbulent energy star formation is delayed and only small stars will form (see appendix A).

The quantity Q_t in equation (11) depends on q_t (equation 15) and we may write
$$q_t = \frac{k\theta}{mt_c} D(u/c). \tag{43}$$

The dissipation function, $D(u/c)$, is calculated and tabulated before the integration begins and values are found from the table by parabolic interpolation. The value of β (equation 16) is a variable parameter of the programme and typical values have been in the range 0.1–1.0.

The steps in the computer programme STARFORM were as follows:

(i) Integrate equations (8′) and (11) forward in time by a standard four-step Runge–Kutta procedure. The total simulated time step, H, for which this is done is such that
$$\Delta\epsilon < (\Delta\epsilon)_c, \quad \Delta\dot{R} < (\Delta\dot{R})_c \quad \text{and} \quad \Delta R < (\Delta R)_c$$
where $(\Delta\epsilon)_c$, $(\Delta\dot{R})_c$ and $(\Delta R)_c$ are preset maximum allowed changes.

(ii) As soon as u reaches the value which gives $\phi > \phi_{max}$ for a head-on collision then the average value of t_c in the interval H is used to compute $\dot{S}$ from equation (40). The number of stars produced in the interval H is taken as $\dot{S}H$, each of mass M_s (equation 41). Because of varying conditions of collision of the elements, giving different values of η and ϕ, stars will be formed with a range of masses but no account has been taken of this.

These steps are repeated until the end of the star formation. This will probably happen in an actual stellar cluster when radiation from the stars begins to break up the cloud and so prevent new stars forming (Herbig 1962).

For our present model star formation was terminated either when the stars produced have masses less than $0.07\,M_\odot$, which may be an observable minimum mass although smaller condensations may be formed, or when the total number exceeded some preset limit, usually in the range 400–1000. In fact this latter limit was rarely invoked.

A large number of calculations have been made with different starting conditions. The results of three of these (parameters in table 1) are shown in figures 7, 8 and 9.

Figures 7*a*, 8*a* and 9*a* show the variations with time of the radius, density and turbulence of the cloud. The fairly constant rate of decrease of radius is common to all the calculations. In an unhindered gravitational collapse there is an acceleration of the collapse. However, in our case, although the temperature has been kept constant, there is a steady build up of turbulent energy which serves to inhibit a runaway collapse.

In constrast to, and related to, the steady collapse speed there is an accelerating increase in density and also of the Mach number of the turbulence. The onset of high turbulence induces star formation and the time at which this happens is shown in the figures. There is a low rate of star formation prior to time shown but any rate less than 0.5 stars per 1 Ma has been ignored.

Figures 7*b*, 8*b* and 9*b* show the number of stars formed per interval of 2.5×10^5 years and also the range of star masses produced within that interval. In these calculations the first stars produced at a significant rate have masses of about 1.3–1.4 $M_\odot$; in some other calculations the first stars produced are less or more massive than those obtained here but it is rare for the initial mass to be outside the range 1–2 $M_\odot$.

As the process continues so the mass of the new stars becomes less but the rate of formation increases. This is consistent with what we see in the lower branch of figure 1*a* and also in the rate-of-formation against time relation shown in figure 1*b*. The calculated rates of formation agree well with observation down to about 1 Ma from the end of the process but, thereafter, the model gives up to four times the observed rate.

The mass distributions given in figures 7*c*, 8*c* and 9*c* are remarkably consistent in giving a mass index in the range -2.5 to -2.7 and this turns out to be an inherent property of the model (appendix A). There is, nevertheless, an important difference between the mass distributions from calculation and from observation. Firstly, the calculations give no stars more massive than about 1.35 $M_\odot$, which corresponds to most of the range (but not most of the stars) in figure 1*c*. The second difference is that the calculations do not give a fall off in frequency for stars of smaller mass and this is linked with what we have previously noted about the too-great predicted rate of star formation in the later stages.

One can reconcile the calculations and observations by, what is admittedly, some *post hoc* reasoning. For a γ of $\frac{5}{3}$ it has been shown that with $\phi_{\max} = 4$ no collision of elements can be too violent to form a star. Nevertheless, for a very violent collision there will be considerable heating and therefore the cooling time may not be completely negligible with respect to the reexpansion time as has been assumed. This is not only because cooling must take place from a higher temperature but, of greater significance, because the reexpansion velocity will depend on the enhanced speed of sound in the heated gas. Consequently the rate of star formation for high turbulent velocities could well be less than that predicted by equation (40) and may even give a diminution of rate with increasing u/c for large u/c as is true for $\gamma < \frac{5}{3}$ (figure 6).

When the present theory of star formation is developed further an attempt will be made to quantitatively include this effect. For now it seems fair to say that, bearing in mind the rather simple nature of the model, the agreement with observation is seen to be satisfactory, except for the formation of the upper branch of the mass-age diagram.

11. Massive stars: initial considerations

When a protostar is first formed and separates from the extraneous material of the colliding turbulent elements it has a density $\rho_2 = \phi\rho_1$ where ρ_1 is the background density and ϕ the compression ratio. Larsen (1969) has examined the collapse of a protostar of one solar mass starting with a density *ca.* $10^{-16}\,\mathrm{kg\,m^{-3}}$ and $\theta = 10\,\mathrm{K}$, and his model seems to be the one most appropriate to our present needs. Its free-fall collapse time is about 7 Ts and the central region of the protostar does collapse on about this timescale. However, the outer material collapses much more slowly and when Larsen's star appears on the Hayashi track it is with radius about $2R_\odot$ and with luminosity $1.3L_\odot$.

As long as the protostar is moving within the cloud it may accrete material and we are going to investigate the accretion process to see whether it can lead to stars of large mass.

There are two basic types of accretion mechanism. The first considers the external medium moving relative to the star at speed V and assumes that all the material deflected by the star's gravitational field which strikes its surface is accreted (Eddington 1926). This leads to an accretion rate for a star of radius r

$$\frac{\mathrm{d}M}{\mathrm{d}t} = \pi r(r+2GM/V^2)\,\rho_1 V, \tag{44}$$

corresponding to an accretion radius.

$$r_a = \{r(r+2GM/V^2)\}^{\frac{1}{2}}. \tag{45}$$

The second mechanism also takes as accreted some material which describes hyperbolic orbits about the star and forms a high-density accretion column along the downstream axis. A formula suggested by Bondi (1952) for this type of accretion is

$$\frac{\mathrm{d}M}{\mathrm{d}t} = 2\pi G^2M^2\rho_1(V^2+c^2)^{-\frac{3}{2}}, \tag{46}$$

corresponding to accretion radius

$$r_b = \surd 2GMV^{-\frac{1}{2}}(V^2+c^2)^{-\frac{3}{4}}. \tag{47}$$

In any particular situation the accretion radius to use is whichever is the larger of r_a and r_b.

We begin by considering a star formed at position A of figure 7. The initial characteristics of this protostar are:

$$M = 1.35\,M_\odot; \quad \rho_2 = 3.62\rho_1 = 1.77\times10^{-17}\,\mathrm{kg\,m^{-3}};$$
$$r_I = 3.3\,\mathrm{Pm}\dagger; \quad \theta = 8\,\mathrm{K}, \quad c^2 = 9.2\times10^4\,\mathrm{m^2\,s^{-2}}.$$

For such a protostar $r_a > r_b$ for any reasonable values of $V(\approx 1\,\mathrm{km\,s^{-1}})$ so that equation (44) is the correct one to use. However, the escape speed from the protostar, V_e, is $3.2\times10^2\,\mathrm{m\,s^{-1}}$ and with the values of c^2 which pertains there will be a heavy spontaneous loss of material, rather like the loss of a temporary atmosphere from a low-mass planet. While this will give rise to a substantial loss of surface material, the bulk of material in the protostar will collapse.

Another effect leading to loss of protostar material may be described as 'abrasion'. Accreted material falls on the surface with speed $(V^2+V_e^2)^{\frac{1}{2}}$ and shares energy with protostar material. Since V^2 is many times greater than V_e^2 a nett loss of material may ensue. We can think of this at a molecular level. An incident molecule will share its energy with molecules near the surface of the star. Several stages of interaction will be required to thermalize the energy of the incident molecule and the early interactions will give rise to several molecules with velocity well above escape velocity. If any one molecule happens to move off in a suitable way and escape then the loss of mass equals the gain. If two or more molecules escape then the loss exceeds the gain.

The combined evaporation and abrasion effects should depend strongly on just where the gas stream falls on the surface. Stellar material evaporating from the surface directly facing the oncoming cloud material will interact with it and so be forced back towards the star. There will be no such hindrance to escape, and indeed there will be abrasion assistance, where the material falls on the surface in a direction making a large angle to the normal.

Our conclusion, based for the most part on intuition, is that for a tenous protostar there will be little mass gain by accretion and there may even be a nett loss of mass.

It might be expected that the abrasion loss will become insignificant when the protostar has collapsed to a radius, r_{ab}, where

$$2GM/r_{ab} \approx V^2. \tag{48}$$

† 1 Pm = 10^{15} m.

PHILOSOPHICAL TRANSACTIONS OF THE ROYAL SOCIETY A MATHEMATICAL, PHYSICAL & ENGINEERING SCIENCES

For our present protostar, taking V to be of the same order as u(2 km s^{-1}) we find 90 Tm. At this stage the collapse will be fairly rapid but, in any case, the star is close to the state where $r_b \approx r_a$ and therefter accretion will be governed by equation (46).

12. Star growth: a model

The various accretion theories which have been developed assume that the star is moving relative to a quiescent cloud. Consideration of accretion in a turbulent cloud leads us to the following set of propositions.

(i) Streams of material falling on the protostar surface at angles to the normal which are not too great will be directly and immediately accreted.

(ii) Streams of material falling on the surface at a high angle to the normal may 'bounce' and only return to the surface after some time, if at all.

(iii) The accretion column forms in the wake of the protostar and time must elapse before it joins the star.

(iv) Any material not immediately accreted suffers some risk of being disturbed by turbulence and may therefore only partially be accreted.

(v) Because of turbulence, systematic relative motion of cloud material and star is only possible within a certain distance of the star.

Propositions (i)–(iv) means that the accretion efficiency of a stream of material will depend on its distance from the central axis. A stream close to the axis might be accreted with almost unit efficiency while a stream contributing to a remote region of the accretion column might provide very little accreted material.

In consideration of proposition (v) we note that the coherence length in our cloud is $2R_J$. Consequently if we look at the turbulent velocities $\boldsymbol{u}_1$ and $\boldsymbol{u}_2$ at two points a distance $2R_J$ apart we expect

$$\overline{|\boldsymbol{u}_1-\boldsymbol{u}_2|^2} = 2u^2. \tag{49}$$

We now propose that for two points a distance r apart

$$\overline{|\Delta \boldsymbol{u}|^2} = u^2 r/R_J. \tag{50}$$

The distance from the protostar at which a systematic relative motion might be maintained is that at which the expected energy of the random motion is less than some fraction of the systematic energy of the stream. For a unit mass of stream material, assumed to have speed V at an infinite distance from the star, the energy at distance r is

$$\epsilon_r = \tfrac{1}{2}V^2 + GM/r. \tag{51}$$

We now find the maximum distance at which systematic motion can be maintained as the value of r satisfying

$$\frac{r}{R_J}u^2 = \alpha\left(\tfrac{1}{2}V^2 + \frac{GM}{r}\right). \tag{52}$$

The critical distance so found is

$$r_s = \alpha\frac{R_J V^2}{4u^2}\left\{1+\left(1+\frac{16GMu^2}{\alpha R_J V^4}\right)^{\frac{1}{2}}\right\}. \tag{53}$$

When accretion is being influenced by turbulence then the accretion radius, r_c, would be less than r_s for a flow pattern to be established and we write

$$r_c = g\frac{R_J V^2}{4u^2}\left\{1+\left(1+\frac{16GMu^2}{\alpha R_J V^4}\right)^{\frac{1}{2}}\right\}. \quad (54)$$

In numerical work the values of g and α have been taken as 0.1 and 0.6 respectively; the general conclusions which follow are not very sensitive to these values but the values were chosen to give a reasonable match to observation.

When turbulence is not excessive then it may happen that r_c is greater than r_b, the normal accretion radius defined in equation (47). The accretion radius which is used, r_{ac}, is the lesser of r_c and r_b.

There is one other factor which needs to be taken into account and which relates to the difference between the model described here and a non-homogeneous model. At all times, and especially in the later stages of collapse, the centre of a real cloud would have density higher than that of the cloud as a whole. The density should be only a function of time but also of position in the cloud and we write

$$\rho_1' = f\rho_1, \quad (55)$$

where f represents the enhancement factor of density in the vicinity of the accreting star. In the later stages of collapse this enhancement can be two or three orders of magnitude (Disney *et al.* 1969) although we shall never use such extreme values.

The final mass of the star is now given as

$$M_f = M_0 + \int_{t_0}^{t_f} \pi r_{ac}^2 \rho_1' V\,dt, \quad (56)$$

where M_0 is the initial mass of the star and t_0 and t_f the initial and final times. The actual value of the integral requires many quantities to be specfied as functions of time although the only ones available to us from the calculations giving figures 7–9 are ρ_1, u and R_J.

Calculations have been made starting from various points along the initial mass-development line shown in figure 7*b*. Along each accretion line, shown in figure 10, the values of V/u and f have been kept constant although in practice these values would be expected to vary as the accreting star moved at different speeds through different parts of the cloud material. We may regard the shown accretion lines as rough guides to possible paths of mass development with substantial deviations above and below the lines possible and corresponding to fluctuations in f and V/u.

The calculations were made for four values of f, (1, $10^{\frac{1}{3}}$, 10, $10^{\frac{2}{3}}$) and five values of V/u, (3^{-1}, $3^{-\frac{1}{2}}$, 1, $3^{\frac{1}{2}}$, 3). The central condensation of the cloud would increase as it collapses so the maximum value of f is permitted only with accretion lines starting at later times; the total range of V/u is considered to be available at all times. Although the central condensation may become very high, f, which is a mean value over the accretion time, is fairly restricted. In the later stages of the collapse of the cloud stars will be tending to move faster in a cloud of smaller dimensions and there is very little likelihood that the star could stay within the region of highest density for an extended period.

A star beginning at point A with mass 1.35 $M_\odot$ and accreting along AC with $V/u = 3^{-\frac{1}{2}}$ and $f = 10^{\frac{1}{3}}$ would finish after 4.5 Ma with a mass 2.50 $M_\odot$. However, if at the point X the value of f became and stayed at $10^{\frac{2}{3}}$ it could thereafter accrete along the path XJ.

On the basis of this picture we might find an accreting star at some stage of development anywhere in the region roughly delineated by the points AMJXA in figure 10. What we do not know is how to compare these results with those shown in figure 1*a*. The essential problem with making a comparison between theoretical and observed mass–time relations in a cluster is knowing exactly what stage of the theoretical calculation corresponds to the accepted zero-age observation. The observational zero-age is based on a hypothetical point in the H.–R. diagram obtained by extrapolating along the constant-temperature part of the Hayashi track and corresponding to infinite luminosity (Iben & Talbot 1966). However, there is a lack of knowledge of the evolutionary track of a rapidly accreting star in the H.–R. diagram. If there are rapidly accreting stars

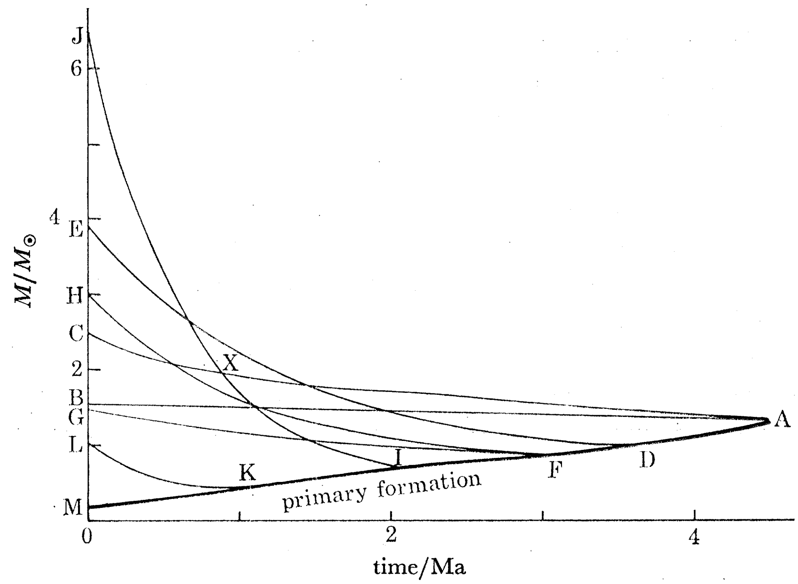

FIGURE 10. Accretion lines for the model illustrated in figure 7:

line	$M_0/M_\odot$	$M_t/M_\odot$	f	V/u
AB	1.35	1.65	1	$3^{-\frac{1}{2}}$
AC	1.35	2.50	$10^{\frac{1}{2}}$	$3^{-\frac{1}{2}}$
DE	0.97	3.89	10	$3^{-\frac{1}{2}}$
FG	0.80	1.50	10	3^{-1}
FH	0.80	3.00	10	$3^{-\frac{1}{2}}$
IJ	0.71	6.64	$10^{\frac{3}{2}}$	$3^{-\frac{1}{2}}$
KL	0.42	1.01	$10^{\frac{3}{2}}$	$3^{-\frac{1}{2}}$

in a young stellar cluster, but their characteristics are being judged relative to a non-accreting model, then assumptions about their mass and age are invalid. The problem of the evolution of a star with mass loss has received some attention (for example Ezer & Cameron 1971) because of its relevance to T-tauri mass loss. The corresponding problem with mass accretion seems not to have been treated in any detail although von Sengbusch & Temesvary (1966) have considered the implication of rapid accretion on the Hayashi theory and they suggest that the theory may need substantial modification under this condition.

One possible hypothesis is that the time of origin of a star, as determined by its position in the Hertzsprung–Russell diagram, is to be measured from when it ceases to accrete rapidly. With this assumption any accretion lines of small slope will not be generators of mass-time points except near their beginning points but mass-time points may arise anywhere on an accretion line of high slope. On this basis it seems possible to interpret figure 1*a* in terms of the results shown in figure 10.

There are, of course, many complications in comparison of our present results with the observations in young stellar clusters. For example, we do not know how a star behaves if it has ceased to accrete, become firmly established on a Hayashi track, and then begins again to accrete rapidly. It is, in fact, quite possible that once the star has become a highly luminous object it will cease to accrete at all.

For a dust grain the ratio of the force on it due to radiation compared to that of gravity is

$$Z = \frac{3L_* \sigma}{4\pi G M c_1 \rho a^3}, \tag{57}$$

where L_* is the luminosity of the star, c_1 the speed of light and ρ, a and σ are respectively the density, radius and absorption cross section of a grain. With $L_* = 5L_\odot$, $\rho = 2 \times 10^3\,\mathrm{kg\,m^{-3}}$ and other quantities as given previously we find

$$Z = 70\sigma/\pi a^2. \tag{58}$$

For radiation from a source at 3000 K or higher the peak wavelength is about 1 μm and the absorption efficiency ($\sigma/\pi a^2$) will not markedly differ from unity (Gaustad 1963). Although the grains form only 1–2 % of the total mass of the cloud they are so strongly coupled to the gas that the gravitational field of the star may be partly or even totally nullified.

There are still many observed features which remain to be explained, in particular the gap which appears between the two streams of mass development in figure 1*a*. Nevertheless it seems fair to say that the major features of the observations have been explained in terms of the present model.

13. Stellar rotation

A property of stars for which there is no generally agreed explanation is the way in which their rotational equatorial speeds vary with spectral type, as is shown in figure 11. For stars later than about F5 equatorial speeds are low. There is a sharp increase in equatorial speeds for stars earlier than F5 and there seems to be a peak at about the B5 region. We shall now see how the present model can be reconciled with those observations.

First we consider the collision of two turbulent elements, which are really streams of gas in the cloud, which are coming together to form a star. In figure 12*a* these are portrayed as streams of equal mass, speed and lateral dimension meeting head on a centre-to-centre collision. If the speed of the gas is uniform across both streams then it is obvious that there will be no angular momentum in the resulting star. This conclusion is maintained even if one stream contains more mass or is moving with a higher speed.

Now we imagine, as in figure 12*b*, that the streams still move to a head on collision but that they are offset by an amount z. The offset distance cannot be too great otherwise the condition expressed by equation (31) will not be satisfied. The two streams now have a nett angular momentum amounting to zu per unit mass but none of this will be associated with the protostar; for the compressed material there will be no attendant angular momentum. This is all contained in the peripheral uncompressed material which plays no part in star formation.

Next we consider the case as in figure 12*c* where the collision is between two oblique streams; indeed when the speeds of the turbulent elements are high then, for star formation, it is advantageous to have an oblique collision to keep the heating of the compressed material down to a suitable level (§ 10). In figure 12*d* the situation of figure 12*c* is redepicted but this time from the point of view of the centre of mass of the system. It is seen to be equivalent to the head on collision of two streams, with some offset of centres and perhaps with differing speeds and densities, but the conclusion about angular momentum is the same as before. This is an important result: *the interaction of two uniform streams of gas gives no systematic contribution to the angular momentum of the compressed region so produced.*

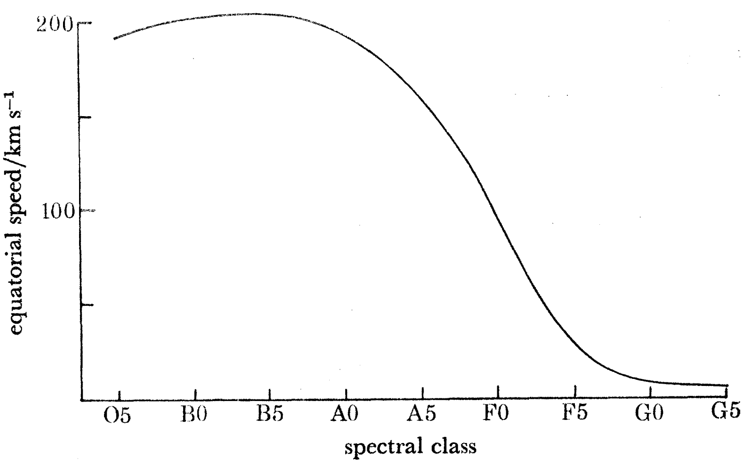

FIGURE 11. The variation of the average equatorial speed with spectral class of star.

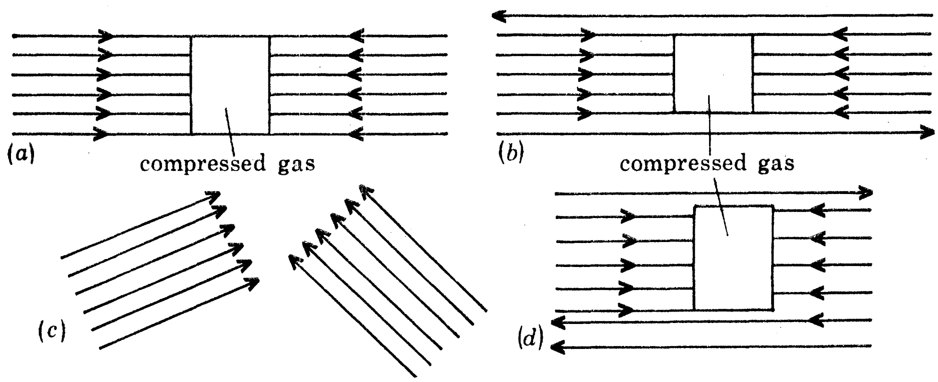

FIGURE 12. (*a*) Head on collision of two streams of gas with similar densities and speeds. (*b*) An offset collision. All the angular momentum of the system is associated with uncompressed material. (*c*) Two interacting streams of gas with non-parallel motions. (*d*) The situation shown in (*c*) referred to the centre of mass of the gas streams.

In the above discussion the assumption has been that the streams are uniform across their interacting cross sections. That this is so, or approximately so, cannot be formally justified and there seems to be no well established theory for the properties of streams of matter in a turbulent cloud. We see from figure 4 that the condition of uniform motion is necessary only in the central part of the streams and intuitively this seems to be not unreasonable. However, there is another mechanism which can give rise to low angular speed for a newly formed protostar. The newly formed star will have a density only a few times greater than that of the surrounding medium in which it is embedded. This will imply a strong viscous coupling of protostar to medium: indeed, the abrasion effect referred to in the previous section implies this. As the star condenses it will be gaining material by direct impact with accretion radius r_a (equation 45) and also losing material

PHILOSOPHICAL TRANSACTIONS OF THE ROYAL SOCIETY A MATHEMATICAL, PHYSICAL & ENGINEERING SCIENCES

by abrasion and evaporation. While these effects are in balance the intrinsic angular momentum of the protostar surface material would be approximately that of the acquired material.

We can estimate the condition for a balance of abrasion and accretion in the following way. The material from the central region of the accretion cross section, of radius r_{ac}, will be accreted whilst outer material will abrade the star. If the speed of onfall of the material on the stellar surface is

$$V_f = mV_e \tag{59}$$

then, by sharing its energy with star material, material in the outer region can eject to infinity up to (m^2-1) times its own mass. For equality of accretion and abrasion the accretion part of the cross section will have radius r_p given by

$$r_p^2 = \frac{m^2-1}{m^2} r_{ac}^2. \tag{60}$$

For the stellar radii we are dealing with the accretion radius is given by equation (45) or, from condition (59),

$$r_{ac}^2 = r^2 + \frac{2GM}{V^2} r,$$

$$= \frac{m^2}{m^2-1} \frac{4G^2M^2}{V^4}. \tag{61}$$

This gives

$$r_p = \frac{2GM}{V^2} \tag{62}$$

and the value of r_p is the appropriate one for estimating the angular momentum of the accreted material. We see that the value of r_p is independent of the choice of m. The assumption about the abrasion of outer material will break down when m becomes small enough, that is when the star has a small radius, but while the assumption is valid equation (62) will hold.

The angular momentum per unit mass of accreted material is, by equation (B 5) (appendix B),

$$H_m = \frac{G^2M^2u}{8R_J V^4}. \tag{63}$$

If this is the intrinsic angular momentum of stellar equatorial material, which persists when it collapses to its main sequence radius r_*, then the final equatorial speed of the star is given by

$$V_{eq} = \frac{G^2M^2u}{8R_J V^4 r_*}. \tag{64}$$

For the model which gave figure 7, when $M = M_\odot$ then $u = 1.65\,\text{km}\,\text{s}^{-1}$ and $R_J = 8\,\text{Pm}$. With $r_* = R_\odot$ and V between $2\,\text{km}\,\text{s}^{-1}$ and $4\,\text{km}\,\text{s}^{-1}$ the value of V_{eq} is between $41\,\text{km}\,\text{s}^{-1}$ and $2.6\,\text{km}\,\text{s}^{-1}$, well within the range of late-type stars.

To supplement the above-mentioned cloud-star coupling there are other mechanisms which can lead to loss of angular momentum of a young protostar. For example, Hoyle (1960), has postulated that angular momentum transfer can be effected by magnetic coupling. This requires the material to be sufficiently conducting (ionized) for the magnetic field to be frozen into it, or at least partially so. The coupling will only be operative when the medium is moving slowly, which implies a comparatively low density. Hoyle postulated that the coupling would be maintained down to a high stellar density but this is because his estimate of the available magnetic field was unrealistically high (Woolfson 1969). Observation of the polarisation of hydroxyl maser radiation from star-forming regions indicates fields not greatly in excess of 10^2 nT (Cook 1977).

Another mechanism which has been suggested for the removal of angular momentum from young stars involves the shedding of material which takes place in the T-Tauri stage of the star's development.

All in all the idea that a non-accreting star may have little associated angular momentum seems quite tenable. The basic mechanism of star formation gives a tendency for low angular momentum in the first place and coupling to the medium, by one means or another, during the initial stages of collapse plus possible T-Tauri emission effects could reduce the initial angular momentum still further.

We now turn our attention to the angular momentum of stars which have had substantial gain of mass by accretion. When the calculations were carried out which included the accretion lines shown in figure 10 the angular momentum of the accreted material was also found. From the results in appendix B the total angular momentum may be found as

$$H = \frac{1}{32}\int_{M_0}^{M_f} r_{ac}^2 \frac{u}{R_J}\,\mathrm{d}M. \tag{65}$$

This result would be in error in that it does not take into account the vector nature of angular momentum. As the star accretes it moves from one turbulent region to another and the angular momentum contributions from each region add vectorially. Thus we should have

$$\bar{H} = \left\{\sum_{k=1}^{n} H_k^2\right\}^{\frac{1}{2}}, \tag{66}$$

where H_k is the magnitude of the acquired angular momentum in turbulent region k.

The average time taken to traverse a turbulent region, t_r, is given by

$$t_r = 4R_J/3V, \tag{67}$$

ignoring the variation of the right hand side quantities with time. This result comes about by taking the mean path through a spherical turbulent region of diameter $2R_J$ as $\frac{4}{3}R_J$. Proper allowance is made for the vector addition of H by computing

$$H = \left\{\int_{t_0}^{t_f} t_r \left(\frac{\mathrm{d}H}{\mathrm{d}M}\right)^2 \left(\frac{\mathrm{d}M}{\mathrm{d}t}\right)^2 \mathrm{d}t\right\}^{\frac{1}{2}} \tag{68}$$

where $(\mathrm{d}H/\mathrm{d}M)$ and $(\mathrm{d}M/\mathrm{d}t)$ are given by equation (B 5) and by the integrand of equation (56) respectively.

Before we investigate this equation to see what it will yield in numerical terms it will be useful to see what observation tells us about the angular momentum of stars as a function of their mass.

The observation of a star of mass M_* and radius R_* gives its equatorial speed, V_*, and assuming a rigid rotation of the star this translates into an observed angular momentum

$$H_* = \alpha_* M_* R_* V_*, \tag{69}$$

where α_* is the moment of inertia factor, that is the moment of inertia

$$I = \alpha_* M_* R_*^2. \tag{70}$$

To estimate values of α_* the results for the density distribution within stars given by Chandrasekhar (1939) were used (appendix C). The values of M_*, R_*, V_* and α_* derived from various published sources are given in table 2 for stars above one solar mass. The associated angular momenta, H_*, are shown in figure 13 as a function of M_* and it will be seen that except at the lower end of the mass range a law of the form

$$H \propto M^{2.1} \tag{71}$$

appears to hold.

Table 2. Estimated values of M_*, R_*, α_* and V_*

star type	$M_*/M_\odot$	$R/_*R_\odot$	α_*	$V_*/(\text{km s}^{-1})$	$H_*/(\text{kg m}^2\text{ s}^{-1})$
O5	39.8	17.8	0.131	192	2.49×10^{46}
BO	17.0	7.59	0.118	203	4.33×10^{45}
B5	7.08	3.98	0.084	211	6.99×10^{44}
AO	3.55	2.63	0.064	192	1.61×10^{44}
A5	2.19	1.78	0.055	161	4.83×10^{43}
FO	1.78	1.35	0.053	98	1.75×10^{43}
F5	1.41	1.20	0.051	30	3.62×10^{42}

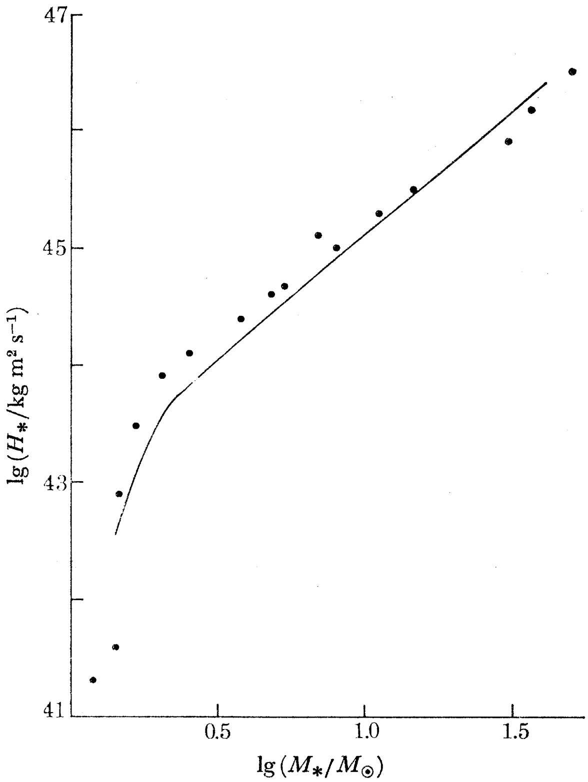

Figure 13. The observed relationship between the angular momentum of a star H_* and its mass M_* (full line). The theoretical points are derived from the model which gives figure 7.

Figure 13 also shows a representative (and randomly chosen) sample of results calculated from equation (68). The agreement between observation and theory is surprisingly good and this even includes the departure from the straight line relationship observed for the lower masses.

It turns out that most accretion takes place at the end of the accretion period because the density of the cloud increases with time. If most mass, and therefore angular momentum, is acquired in one turbulent region then the vector addition feature can be ignored and equation (65) is valid. At the end of the accretion period it is likely that the accretion radius is limited by turbulence, as given by equation (54). We then find the general form of the relationship giving H as

$$H = A\int_{M_0}^{M_f} \{1+(1+BM)^{\frac{1}{2}}\}^2 \, dM$$
$$= \tfrac{1}{2}AB(M_f^2 - M_0^2) + \frac{4A}{3B}\{(1+BM_f)^{\frac{3}{2}} - (1+BM_0)^{\frac{3}{2}}\} + 2A(M_f - M_0). \quad (72)$$

For large M_f this gives $$H \propto M_f^2,$$

which agrees with the calculated results shown.

While not too much should be read into the precise numerical agreement – there are too many uncertainties in the model for that – what does seem significant is the similarity in the form of relation between H and M even to the extent that the power-law relation breaks down in a similar way for low mass stars.

14. Frequency of planetary systems

Observations of the proper motions of some nearer stars suggest that they may have invisible planetary companions. If this is so, and planetary systems are common, then it imposes a fairly heavy constraint on any theory of the origin of the solar system.

In the capture theory (Woolfson 1964; Dormand & Woolfson 1971, 1974, 1977) planets are formed by the capture of material from a light, diffuse star by tidal forces during an encounter. The capturing star is compact and, for planetary condensation to be possible, the encounter must take place with a centre to centre distance $1\frac{1}{2}$ to 2 times the radius of the diffuse donor star.

The capture theory has always assumed that such an encounter would take place within a young stellar cluster, and the 1971 paper gave an estimate of the frequency of such encounters. Reference was also made to work by Aarseth (1968) who has used numerical methods to study the evolution of a cluster and has concluded that encounters would be common, many of them leading to the formation of binary systems.

The present model for star formation gives a period at the end of the star-formation process when stars in the range 0.1–$0.5\,M_\odot$ are produced on a short time scale and in great profusion. At this stage the whole cloud will be collapsing rapidly with its radius falling to 10 Pm or even less.

It might be thought that the capture theory mechanism could operate to produce planets as soon as a diffuse protostar was formed but this is not so; the protostar must first attain a density such that a captured fragment of itself could collapse to form a planet. Thus, from Jeans's criterion, we find that to produce a planet of mass five times that of Jupiter from a protostar of mass $\frac{1}{4}M_\odot$ requires a stellar radius less than about 25 Tm.

We now consider a protostar of mass m and radius r moving with speed W relative to a compact star of mass M. For a passage at nearest distance fr the interaction parameter, D, is given by

$$D^2 = (fr)^2 + 2G(M+m)frW^{-2}, \quad (73)$$

and the interaction cross section for a nearest approach between $f_1 r$ and $f_2 r$, $(f_1 > f_2)$, is

$$\pi(D_1^2 - D_2^2) = \pi(f_1^2 - f_2^2)\,r^2 + (f_1 - f_2)\,2\pi G(M+m)\,rW^{-2}. \quad (74)$$

If the protostar maintains the radius r for a time t then the interaction volume for planetary formation swept out by its passage will be

$$Q = \{(f_1^2 - f_2^2)\,r^2 + (f_1 - f_2)\,2G(M+m)\,rW^{-2}\}\,\pi Vt, \quad (75)$$

where V is the speed of passage through the cloud.

PHILOSOPHICAL TRANSACTIONS OF THE ROYAL SOCIETY A MATHEMATICAL, PHYSICAL & ENGINEERING SCIENCES

With N light protostars the total volume of space swept out for planetary forming interactions is NQ and the probability that a particular condensed star will acquire planets is

$$P = \frac{NQ}{\frac{4}{3}\pi R_{\mathrm{cl}}^3}, \tag{76}$$

where R_{cl} is the radius of the cloud.

During the final stages of the collapse of the cloud turbulent velocities have risen to about $5\,\mathrm{km\,s^{-1}}$ and protostars, formed by the oblique collision of turbulent elements, will have speeds, V, of this order. The more massive and condensed stars produced earlier, which happen to have fallen in towards the centre, as their motions tend to direct them, would also have accelerated to speeds of about $5\,\mathrm{km\,s^{-1}}$ and this gives an estimate for W of $\sqrt{2}V(\approx 7\,\mathrm{km\,s^{-1}})$. Estimates of other quantities are:

$$f_1 = 2, \quad f_2 = 1.5, \quad r = 20\,\mathrm{Tm}, \quad M = 2\times 10^{30}\,\mathrm{kg}, \quad m = 5\times 10^{29}\,\mathrm{kg},$$

$$t = 10\,\mathrm{Gs}, \quad N = 500 \quad \text{and} \quad R_{\mathrm{cl}} = 10\,\mathrm{Pm}.$$

Substituting these values in equations (75) and (76) gives $P = 2\times 10^{-5}$. Given 10–100 condensed stars within the central cloud region this gives a probability of 10^{-4}–10^{-3} per cluster for the formation of a planetary system.

We should examine these results in the light of general expectations, beliefs and observations about other planetary systems. There is a prevalent view that planetary systems somewhat like the solar system are quite common and this is coupled with the idea that other centres of life probably exist. Whether this is based on evidence rather than man's hopes based on a gregarious instinct is much to be doubted. However, to be reassuring to this wish, the present results do indicate that planetary systems formed by the capture mechanism will be common. With 10^{11} stars in our own galaxy there should be of order 10^6 planetary systems.

Recent observations, summarized in a paper by Abt (1977), suggest that the great majority of stars have invisible comparisons. This may well be true. The very large number of stars of low mass, including perhaps small unobservable mass condensations, predicted by the present model have a comparatively small probability of a capture type interaction but this is because of the limited time they spend as diffuse objects. The amount of time they spend as more compact objects, in the dense environment of the cloud just before it begins to disperse, is much larger. The work of Aarseth (1968) suggests that many of them will become associated with each other and with more massive stars as binary or even more complex multiple systems. There will be a sharp distinction between the mode of origin of this type of system and that of a planetary system and there is no continuum of interaction pattern between the two extremes.

In his paper Abt has noted a range of mass ratios for the components of binary systems and has found a systematic variation of frequency with mass ratio. He concludes that the cut-off in mass ratio is due only to observational difficulties and by extrapolation he deduces the probable frequency of planetary systems. His conclusion is that virtually all stars are multiple systems. The validity of that extrapolation is challenged by the model we are suggesting here. Recently there have been doubts expressed as to the reliability of the observations on which Abt has based his ideas and it seems reasonable, for more than one reason, to discount his conclusions.

Once again it must be stressed that the numerical results given in this section are indicative only. The idea of a homogeneous cloud with a finite boundary is quite unrealistic and it must be considered as a first order approximation. With a more detailed model now under development different numerical results should be found. Nevertheless even changes of one or two orders of magnitude in the numerical value will not change the general conclusions which have been drawn.

15. Conclusion

In the basic idea presented here for the origin of stars in a cluster there is nothing very novel. Clouds of cold gas with turbulent motion are very much the accepted hypothesis for the origin of stellar clusters. Recent observations of water and hydroxyl maser emission are thought to be associated with star formation; hydroxyl maser sources are found coming from regions of typical diameter 0.1–10 Pm with elementary sources, presumably individually forming stars, of radius 0.1–10 Tm. There are Doppler shift velocities recorded from different parts of the cloud with magnitudes of the order of 20 km s^{-1} which are comparable with the turbulent speeds given by the present model at the end of, and just after, the star forming period. A full account of celestial maser sources and their properties is given by Cook (1977). All in all, current ideas, the maser observations and the present model are mutually quite consistent.

The imperfections of the model have been stressed previously. Inevitably, in order to make progress, models are kept as simple as is compatible with reasonably representing the various aspects of the system under investigation. Later, more complex models may be constructed but even with a simple model it is possible to interpret aspects of it in realistic terms. For example, where we have considered a homogeneous model with a sharp boundary moving inwards we know, from other considerations, that there will actually be density variations with, in general, a higher density in the centre. A sensible interpretation of the sharp boundary would be that it represents a surface which contains a large proportion of the mass, say 90 % or so, and this surface might well behave similarly to the boundary of the simple model.

In presenting the results of this paper, and in particular in comparing results from the model with observation, it is important to be clear how the results came about. It would be pleasant to record that, starting from some well-founded initial point, there was a logical and inevitable process which led to the numerical results which compare so well with observation. Unfortunately this was not so. Rather it was that the model was developed with one eye on the observed quantities and when a match between theory and observation was unsatisfactory then the model was examined to see what modification could give better agreement. The details of the model owe more to *post hoc* than to *ab initio* considerations.

A pleasing feature of the model is the significance of F 5 type stars in both the mass-age correlation diagram, figure 1, and also the equatorial speed relation illustrated in figure 11. The concept of accretion growth, as distinct from the original low angular momentum mechanism, gives a simultaneous explanation of the characteristics of two different observed relationships. Incidentally, in respect of angular momentum, there was a departure from the general rule of *post hoc* reasoning. The model gave angular momentum roughly proportional to the square of the mass for the more massive stars and then, and only then, was the relationship found as illustrated in figure 13.

The stellar rotations given by the present model are completely random in direction since they depend on the addition of streams of material coming from various directions. A point of difficulty of many previous models is that their stellar rotation is derived from the angular momentum of a nebula which is itself part of a cloud possessing the intrinsic angular momentum of the galaxy.

PHILOSOPHICAL TRANSACTIONS OF THE ROYAL SOCIETY A MATHEMATICAL, PHYSICAL & ENGINEERING SCIENCES

Such a starting point would tend to give the individual stars of a cluster highly correlated rotations.

Earlier in this paper it was recorded that the theory to be developed would bear a resemblance to the floccule theory described by McCrea (1960). In McCrea's theory the turbulent elements are of planetary size and the stars are synthesized by the combination of many such elements. The difficulty with this idea is that the individual turbulent units are unstable under Jeans's criterion and it is difficult to see how a stable stellar mass can be created. For small bodies, of planetary size or less, it seems more reasonable to ascribe their origin to the break up in some way of a larger body of stellar mass which itself could have formed by the gravitational collapse of low density material. When such material has collapsed to a sufficiently high density then portions of it can form large planets and the concentration of solid material in these, in its turn, can give rise to the rocky bodies of small planetary size and less.

It is claimed that the ideas presented here and elsewhere for the formation of stars, planets and satellites are totally consistent with observation and can be linked to simple and well understood dynamical mechanisms, including tidal interaction. Again the probabilities of the events described, as deduced from normal statistical principles, give no cause for concern.

The author wishes to express gratitude to the referee of an earlier version of this paper for pertinent criticism and a number of constructive suggestions. These led to substantial modification and improvement of the sections dealing with accretion and angular momentum and beneficial changes in many other sections.

Appendix A. Basic characteristics of the model

The mass of stars first formed and the mass index have been found to vary comparatively little with different sets of input parameters. That this should be so can be confirmed from the general form of the equations used.

When stars are being produced in reasonable numbers $\dot{R}$ is very small and turbulent energy greatly exceeds the thermal energy of the cloud. Thus, from equation (8) we have

$$R \approx \tfrac{3}{5}GM/\epsilon_c, \tag{A 1}$$

where ϵ_c is the value of u^2 when star formation begins. From R we find the mean density of the cloud and then, from (37), the mass of a turbulent element. This leads to

$$M_c = \{3c^2/\gamma\epsilon_c\}^{\frac{3}{2}}\,M. \tag{A 2}$$

For star formation to begin we need $\epsilon_c \approx 50c^2$ and we can see that M_c is independent of the cloud temperature and is given by

$$M_c \approx 7 \times 10^{-3}\,M. \tag{A 3}$$

The mass of the first star produced is, from (41), about $0.16\,M_c$ or $\approx 10^{-3}\,M$. With $M = 3 \times 10^{33}$ kg this corresponds to about $1.5\,M_\odot$. This will be an overestimate since the value of R given by (A 1) is too large. The mass of the first stars does strongly depend on the total mass of the cloud. The masses used in these calculations were taken on the basis of having a few times the total expected mass of stars. However, we may also note that a Jeans critical mass for a hydrogen cloud of density 10^{-20} kg m^{-3} and $\theta = 10$ K is 2.4×10^{33} kg and a wide variation in the mass of clouds giving a galactic cluster may not occur. The final number of stars in a cluster may depend less on the initial mass of the cloud than on the time of appearance of the first O or B star which will disperse the cloud.

To investigate the mass index given by the model we shall first consider the terms on the right hand side of

$$\frac{dS}{dt} = \tfrac{1}{2}N\beta' P(u/c)/t_c. \tag{40}$$

We have, approximately,

$$N \propto M_*^{-1}, \tag{A 4}$$

where M_* is the mass of the stars being formed and from (39) and (38) we find for $u \gg c$ that

$$t_c \propto \rho^{-\frac{1}{2}}. \tag{A 5}$$

It is difficult to find a simple expression for $P(u/c)$ but

$$P(u/c) = a + b\epsilon^{\frac{1}{2}} \tag{A 6}$$

will fit reasonably well over the range of interest for $\gamma = \frac{5}{3}$.

In the turbulence equation (11) the right hand side is usually dominated by the first term so that, ignoring Q_t, we may deduce

$$\epsilon \propto R^{-2}. \tag{A 7}$$

Finally we use

$$M_* \propto \rho^{-\frac{1}{2}}, \tag{A 8}$$

and

$$\rho \propto R^{-3}, \tag{A 9}$$

to find that

$$\frac{dS}{dt} = aM^{-2} + bM^{-\frac{8}{3}}. \tag{A 10}$$

Since we are interested in the number of stars per unit mass range we write

$$\frac{dS}{dt} = \frac{dS}{dM_*}\,\frac{dM_*}{dR}\,\frac{dR}{dt}. \tag{A 11}$$

It is readily found that

$$\frac{dM_*}{dR} \propto M_*^{\frac{1}{3}} \tag{A 12}$$

and we have seen in figures 7*a*, 8*a* and 9*a* that dR/dt is sensibly constant over the period of star formation. The reason for this is that the collapse of the cloud is not so much gravity controlled as turbulence controlled. If turbulence is low then collapse will accelerate, and turbulence is generated as in equation (11). The turbulent pressure then slows down the collapse and less turbulence is generated. This negative feedback mechanism makes the model particularly insensitive to the initial turbulence fed into the system as long as it is not too little. Excessive turbulence is quickly *removed* by dissipation and cooling but it can only *grow* by the collapse of the cloud. With too little initial turbulence the first stars are produced with a high cloud density and therefore with low mass.

Accepting that dR/dt is constant we find from (A 10), (A 11) and (A 12) that

$$\frac{dS}{dM} \propto aM_*^{-\frac{7}{3}} + bM_*^{-3} \tag{A 13}$$

or, integrating with sensible boundary conditions,

$$S = K_1 M_*^{-\frac{4}{3}} + K_2 M_*^{-2}, \tag{A 14}$$

where K_1 and K_2 are negative and positive quantities respectively. The second term is the dominant one and the effect of the first term is that, if a best match is sought with

$$S = KM_*^\alpha, \tag{A 15}$$

then $\alpha < -2$. Since this type of numerical matching is not commonly met the reader may find it instructive to confirm that $0.9x^{-2.2}$ is a better match than $0.9x^{-2}$ for the function $x^{-2} - 0.1x^{-1}$ in the range $x = 1$–5.

We thus see that a mass index of $-(2+\alpha)$, with α of order 0.5, is an expected outcome of the model.

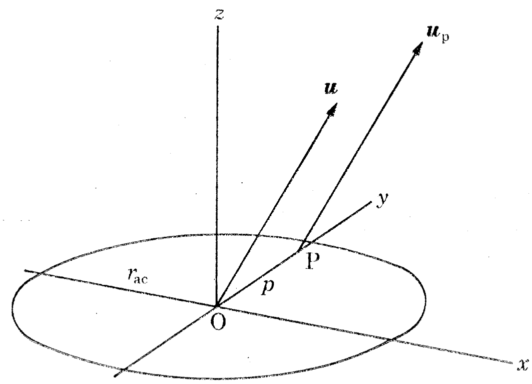

FIGURE 14. The accretion cross section at some distance from the accreting star. $\boldsymbol{V}$ is parallel to Oz and it is assumed that $\boldsymbol{u}$ has constant direction, but not magnitude across the section.

Appendix B. Angular momentum contribution of accreted material

Figure 14 represents the circular cross section of radius r_{ac} through which all accreted material passes on its way to the protostar. The average speed of the material relative to the protostar is V, directed along Oz. The associated angular momentum depends not on V but on the differential speed across the accreting area. Sometimes the growing star will be embedded in a fairly uniform stream and will be acquiring mass but little angular momentum. At other times it will be in the region between turbulent elements and within a very high velocity gradient. We shall take the time average of the gradient as

$$u' = \tfrac{1}{2}u/R_J. \tag{B 1}$$

Over the accretion region, which is usually small in dimension compared with R_J, we may take $\boldsymbol{u}$ to be constant in direction. The axis Ox in figure 14 represents the direction within the plane of no variation of u and hence Oy, orthogonal to Ox, is the direction in the plane in which the gradient varies most rapidly.

If u is the turbulent speed at O then that at P will be given by

$$u_p = u + p(1 - \sin^2\theta \sin^2\phi)^{\frac{1}{2}} u', \tag{B 2}$$

where p is the distance OP and the direction of $\boldsymbol{u}$ is given by the spherical polar angular coordinates (θ, ϕ).

The angular momentum per unit time associated with the material passing through the circular area is

$$\begin{aligned} H_t &= 2\rho V \cos\theta (1 - \sin^2\theta \sin^2\phi)^{\frac{1}{2}} u' \int_0^{r_{ac}} p^2 (r_{ac}^2 - p^2)^{\frac{1}{2}}\,\mathrm{d}p \\ &= \tfrac{1}{8}\pi\rho V r_{ac}^4 u' \cos\theta (1 - \sin^2\theta \sin^2\phi)^{\frac{1}{2}}. \end{aligned} \tag{B 3}$$

PHILOSOPHICAL TRANSACTIONS OF THE ROYAL SOCIETY A MATHEMATICAL, PHYSICAL & ENGINEERING SCIENCES

The angular momentum per unit accreted mass is then

$$H_{\mathrm{m}} = \tfrac{1}{8} r_{\mathrm{ac}}^2 u' \cos\theta (1 - \sin^2\theta \sin^2\phi)^{\frac{1}{2}}. \tag{B 4}$$

To find an average magnitude of H_{m} we need to average the magnitude of the (θ, ϕ) dependent part of (B 4). This can be done on the assumption that θ and ϕ are random variables but this would not be realistic. On the whole θ tends to be small, that is to say that a strong component of V is the actual turbulent flow of the cloud material. An estimate of $\frac{1}{2}$ is used for the magnitude of the (θ, ϕ) term giving

$$H_{\mathrm{m}} = \tfrac{1}{32} r_{\mathrm{ac}}^2 u / R_{\mathrm{J}}. \tag{B 5}$$

Appendix C. Moment of inertia factors of main sequence stars

Chandrasekhar (1939) gives for main sequence stars of various mass the proportion of the radius, ξ^*, within which is contained 90 % of the stellar mass. From this information alone it is possible to make a good estimate of α_*, the moment of inertia factor which is used in table 2.

The value of ξ^* has been used in conjunction with three models of density distribution within the star:

(*a*) $\rho = \rho_0 \exp(-kr)$

(*b*) $\rho = \rho_0 \exp(-pr^2)$

(*c*) $\rho = \begin{cases} \rho_1 & r \leqslant \xi^* R_*, \\ \rho_2 & \xi^* R_* < r \leqslant R_*. \end{cases}$

The values of k, p and ρ_1 are deduced from the value of ξ^* and the values of α_* may then be found by straightforward analysis.

The results are shown in table 3. While the actual values of α_* depends on the model used it turns out that the relative values, as functions of mass, are not very different. In the table this is illustrated by the columns 1.16 $(\alpha_*)_a$, $(\alpha_*)_b$ and 0.893 $(\alpha_*)_c$. Since the theoretical values of H (equation 68) are proportional to several quantities uncertain by much more than 10 % any of the model-derived values of α_* may reasonably be used. In table 2 the values are those deduced by interpolation from the column $1.16(\alpha_*)_a$ in table 3.

Table 3

star	mass/$M_\odot$	ξ^*	$(\alpha_*)_a$	$(\alpha_*)_b$	$(\alpha_*)_c$	1.16 $(\alpha_*)_a$	0.893 $(\alpha_*)_c$
VV Cephei	≈40	0.64	0.113	0.132	0.145	0.131	0.130
V Puppis	18.6	0.615	0.104	0.121	0.133	0.121	0.119
μ_1 Scorpii	12.0	0.58	0.093	0.108	0.118	0.108	0.105
ζ Aurigae	8.1	0.53	0.078	0.090	0.100	0.090	0.089
Sun	1.0	0.40	0.045	0.051	0.066	0.052	0.059
Sirius A	2.3	0.40	0.045	0.051	0.066	0.052	0.059

References

Aarseth, S. J. 1968 *Bull. Astron.* (*Fr*) **3**, 105–125.

Abt, H. A. 1977 *Scient. Amer.* **236**, 4, 96–104.

Aust, C. 1973 In *Recent advances in dynamical astronomy*, eds B. D. Tapley & V. Szebehely, pp. 222–228. Dortrecht: D. Reidel.

Aust, C. 1974 D.Phil. Thesis, University of York.

Bodenheimer, P. 1968 *Astrophy J.* **153**, 483–494.

Bodenheimer, P. 1972 *Rep. Prog. Phys.* **35**, 1–54.

PHILOSOPHICAL TRANSACTIONS OF THE ROYAL SOCIETY A MATHEMATICAL, PHYSICAL & ENGINEERING SCIENCES

Bondi, H. 1952 *Mon. Not. R. astr. Soc.* **112**, 195–204.
Chandrasekhar, S. 1939 *An introduction to the study of stellar structure*. University of Chicago Press.
Chandrasekhar, S. 1960 *Principles of stellar dynamics*. New York: Dover.
Cook, A. H. 1977 *Celestial masers*. Cambridge University Press.
Disney, M. J., McNally, D. & Wright, A. E. 1969 *Mon. Not. R. astr. Soc.* **146**, 123–160.
Dormand, J. R. & Woolfson, M. M. 1971 *Mon. Not. R. astr. Soc.* **151**, 307–331.
Dormand, J. R. & Woolfson, M. M. 1974 *Proc. R. Soc. Lond.* A **340**, 349–365.
Dormand, J. R. & Woolfson, M. M. 1977 *Mon. Not. R. astr. Soc.* **180**, 243–279.
Eddington, A. S. 1926 *The internal constitution of the stars*. Cambridge University Press.
Field, G. B., Goldsmith, D. W. & Habing, H. J. 1969 *Astrophys. J.* **155**, 149–154.
Ezer, D. & Cameron, A. W. 1971 *Astrophys. Space Sci.* **10**, 52–70.
Gaustad, J. E. 1963 *Astrophys. J.* **138**, 1050–1073.
Grzedzielski, S. 1966 *Mon. Not. R. astr. Soc.* **134**, 109–134.
Hattori, T., Nakano, T. & Hayashi, C. 1969 *Prog. theor. Phys. Osaka* **42**, 791–798.
Hayashi, C. 1961 *Publs astr. Soc. Japan* **13**, 450–452.
Hayashi, C. 1966 *A. Rev. Astron & Astrophys.* **4**, 171–192.
Herbig, G. H. 1962 *Adv. Astron. & Astrophys.* **1**, 47–103.
Hoyle, F. 1953 *Astrophys J.* **118**, 513–528.
Hoyle, F. 1960 *Q. JlR. astr. Soc.* **1**, 28–55.
Hunter, C. 1962 *Astrophys. J.* **136**, 594–608.
Hunter, C. 1964 *Astrophys. J.* **139**, 570–586.
Iben, I. & Talbot, R. J. 1966 *Astrophys. J.* **144**, 968–977.
Jeans, J. H. 1902 *Phil. Trans. R. Soc. Lond.* A **199**, 1–53.
Kaplan, S. A. 1966 *Interstellar gas dynamics*, ed. F. Kahn. Oxford: Pergamon Press.
Larsen, R. B. 1969 *Mon. Not. R. astr. Soc.* **145**, 271–295.
Layzer, D. 1964 *A. Rev. Astron. & Astrophys.* **2**, 341–362.
McCrea, W. H. 1960 *Proc. R. Soc. Lond.* A **256**, 245–266.
McNally, D. 1971 *Rep. Prog. Phys.* **34**, 71–108.
Seaton, M. J. 1955 *Annls Astrophys.* **18**, 188–205.
Solomon, P. M. & Wickramasinghe, N. C. 1969 *Astrophys. J.* **158**, 449–460.
von Sengbusch, K. & Temesvary, S. 1966 In *Stellar evolution*, eds. R. F. Stein & A. G. W. Cameron, p. 209. New York: Plenum Press.
Tayler, R. J. 1968 *Rep. Prog. Phys.* **31**, 167–223.
Williams, I. P. & Cremin, A. W. 1969 *Mon. Not. R. astr. Soc.* **144**, 359–373.
Woolfson, M. M. 1964 *Proc. R. Soc. Lond.* A **282**, 485–507.
Woolfson, M. M. 1969 *Rep. Prog. Phys.* **32**, 135–185.

PHILOSOPHICAL TRANSACTIONS OF THE ROYAL SOCIETY A MATHEMATICAL, PHYSICAL & ENGINEERING SCIENCES